unpaired electrons, $(t_2')^1(t_2'')^1$, face the carbonyl ligands, occupying those orbitals of the t_2-like set which remain unperturbed by the bond to hydrogen. The symmetry of this electronic state is $^3A_2$; Jahn–Teller effects of the first order are, therefore, ruled out. One would also expect to find a similar $(e')^1(e'')^1$ $^3A_2$-state of higher energy.

In order to rationalize the two C_s forms, we notice that, besides the above $^3A_2$-states, there are also four "Hückel degenerate" configurations of the type $(e)^1(t_2)^1$. These configurations give rise to states $^3A_1$, $^3A_2$, and ^3E, the last one being Jahn–Teller unstable in the first order. Also, distortions of the second-order cannot be ruled out, because of the expected proximity of these states.

In general, symmetry distortions tend to maximize the "distance" between the unpaired electrons, and such is the case with both C_s conformations: the $(e')^1(t_2')^1$ configuration is distorted by an increase in the angle between hydrogen and the in-plane carbonyl, and the $(e'')^1(t_2'')^1$ configuration decreases the angle between the out-of-plane carbonyls (see Table XV).

However, single-configuration methods cannot describe the two-determinantal states of the C_{3v} conformation, and we do not attempt to characterize the two C_s forms as distortions of any specific states of the full symmetry.

Summary and Conclusions

In contrast with the earlier studies, our work confirms, as distinct energy minima, all of the sterically plausible TBP conformations of the closed-shell form of the hydridocobalt tri- and tetracarbonyls. We find that two fairly different bonding schemes apply to the apical and equatorial hydrogen and that the features of the H–Co bond, as well as the d-orbital splitting, cannot be adequately explained by means of Hückel-type methods.

We come across two classes of triplet states of the tricarbonyl compound: there are tetrahedral d^8-states, similar to those described by Elian and Hoffmann,[19] but we also find the TBP-derived d^7p^1-states. Unlike the tetrahedral states, those of the second class are closely related to the corresponding closed-shell states: one of the unpaired electrons occupies the directional receptor orbital which appeared in lieu of the missing carbonyl, the concomitant differences between the singlet and triplet geometries being fairly small.

We do not regard the relative energies obtained in this work as conclusive. This is especially true of the comparison between open- and closed-shell states, which would be rather meaningless without taking into account the correlation contributions.

The difficult problem of metal–ligand bond lengths also needs to be explored further. Results of some preliminary CI calculations on the $HCo(CO)_4$ molecule confirm the hypothesis that this effect is essentially due to the electron correlation.

Theoretical Analysis of Hydrocarbon Properties. 1. Bonds, Structures, Charge Concentrations, and Charge Relaxations

Kenneth B. Wiberg,*[†] **Richard F. W. Bader,* and Clement D. H. Lau**

Contribution from the Departments of Chemistry, Yale University, New Haven, Connecticut 06511, and McMaster University, Hamilton, Ontario, L8S 4M1 Canada. Received July 11, 1986

Abstract: A theoretical analysis of properties of eight alkanes, four cycloalkanes, seven bicycloalkanes, four propellanes and cubane, tetrahedrane, and spiropentane is presented, based on properties of charge distributions derived from 6-31G* wave functions. Molecular structures are assigned, and a bridgehead bond is found to be present in each of the propellanes. The shortcomings of using density deformation maps or selected sets of orbitals to assign a molecular structure are discussed. Bonds are characterized in terms of a bond order, a bond ellipticity, and the differing extents to which charge is locally concentrated and depleted as determined by the Laplacian of ρ. Bond orders range from 0.7 to 1.3 in the propellanes. Ellipticities of bonds in three-membered rings—a measure of the tendency for charge density to be preferentially accumulated in a given plane—are found to exceed that for the double bond in ethylene. This property and the Laplacian of ρ are used to account for the relative reactivities and structural stabilities of molecules containing small rings. The difference between the bond angle and the corresponding angle formed by bond paths provides a measure of the degree of relaxation of the charge density away from the geometrical constraints imposed by the nuclear framework. The bond path angle is found to exceed the geometrical angle by 23° in spiropentane, 21° in tetrahedrane, 19° in cyclopropane, and −1.5° in cyclohexane. The lowest energy transition densities in the propellanes are used to describe the charge reorganizations accompanying the most facile of the nuclear motions in these molecules.

I. Introduction

The small ring propellanes such as [1.1.1]propellane have unusual structures with "inverted" tetrahedral geometries at the bridgehead carbon atoms, giving them unusual properties and chemical reactivities.[1] We should like to obtain a theoretical understanding of the differences between the properties of these compounds and those of other cyclic hydrocarbons. It has been demonstrated that ab initio molecular orbital calculations are capable of satisfactorily predicting the geometries,[2] enthalpies of formation,[3] vibrational and photoelectron spectra,[4,5] and dipole moments of hydrocarbon molecules in general and of the cyclic

(1) Wiberg, K. B. *Acc. Chem. Res.* **1985**, *17*, 379.

(2) Pople, J. *Mod. Theor. Chem.* **1977**, *4*, 1. Hehre, W. J.; Radom, L.; Schleyer, P. v. R.; Pople, J. *Ab Initio Molecular Orbital Theory*; Wiley: New York, 1986.

(3) (a) Wiberg, K. B. *J. Comput. Chem.* **1984**, *5*, 197. (b) Wiberg, K. B. *J. Org. Chem.* **1985**, *50*, 5285. (c) Ibrahim, M. R.; Schleyer, P. v. R. *J. Comput. Chem.* **1985**, *6*, 157.

(4) Pople, J. A.; Schlegel, H. B.; Krishnan, R.; DeFrees, D. J.; Binkley, J. S.; Frisch, M. J.; Whiteside, R. A.; Hart, R. F.; Hehre, W. J. *Int. J. Quantum Chem., Quantum Chem. Symp.* **1981**, *15*, 269. Hess, B. A., Jr.; Schaad, L. J.; Carsky, P.; Zahradnik, R. *Chem. Rev.* **1986**, 709–762.

† Yale University.

and propellane molecules in particular.[6]   Indeed the synthesis of [1.1.1]propellane[7] was prompted by theoretical calculations which showed that the energy of hydrogenolysis of this propellane is essentially the same as that for cyclopropane or cyclobutane.[6]

All of the above are calculations of the properties of the total molecule. Molecular orbital theory has been less successful at relating these and other properties to the usual chemical concepts—to the properties of the atoms and of the bonds which link them to form the molecule. Attempts have been made to use orbital models to describe the bonding in these compounds.[8-11] A difficulty with such treatments is that one generally uses some subset of the occupied orbitals and thereby incurs the possibility of overlooking important contributions to the total properties of the system from other orbitals. Such procedures require that one make an arbitrary choice of the orbital set (e.g., canonical or localized) as well as of the subset of orbitals to be analyzed. A potentially more promising approach is to use a theory that relates chemical concepts to the total electronic charge density (ρ) as determined by all of the occupied orbitals.[12-15]

The electronic charge density has the additional advantage of being experimentally determinable. While it can be well approximated by ab initio calculations within the orbital theory of electronic structure, the electronic charge density is a physical property of the system and is, therefore, model independent. The usual method of obtaining the charge density from X-ray diffraction data involves the use of the promolecule density—the density obtained by centering a spherical free-atom charge density on each nucleus in the unit cell. The promolecule density is used in fitting the experimental data, and what is obtained directly by this method is the so-called deformation density, the difference between the total experimental density and the promolecule density.[16,17]   When corrected for the effects of vibrational averaging, there is generally good agreement between experimentally determined deformation densities and those obtained from ab initio molecular orbital calculations.[18-20]   The deformation density obtained experimentally for a [3.1.1]propellane derivative, which contains a pair of neighboring inverted carbon atoms as found in all the small ring propellanes, is found to exhibit a relative depletion rather than a buildup of charge between the bridgehead carbons.[21]   The failure of a deformation density map to exhibit the anticipated buildup of charge between a pair of atoms con-
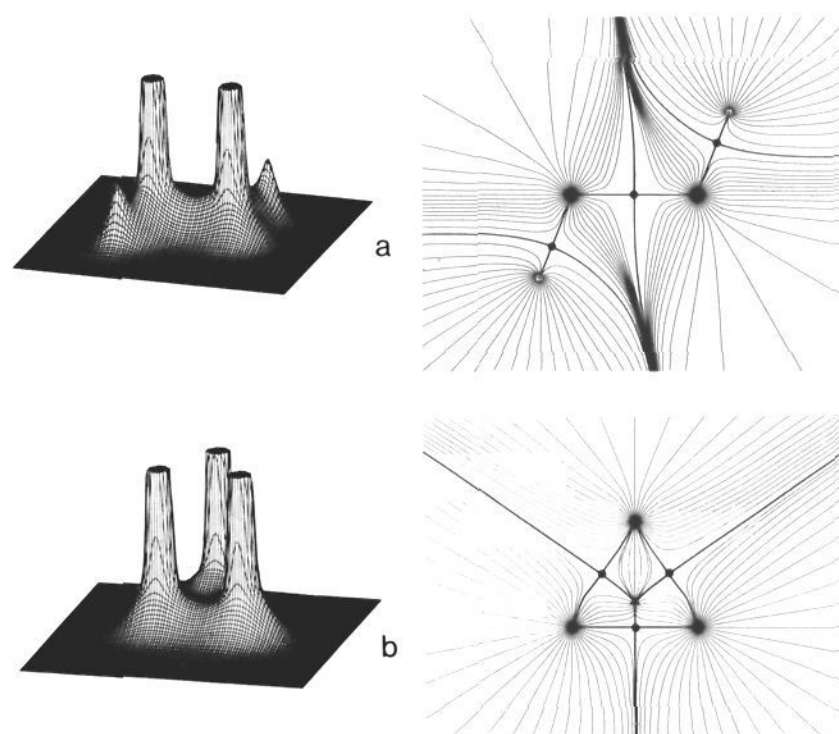

Figure 1. Relief maps of the electronic charge density and representations of the gradient vector field of the charge density in terms of the paths traced out by the vectors $\nabla\rho$ (a) for the plane containing the H–C–C–H nuclear framework of ethane and (b) for the plane of a three-membered ring in [1.1.1]propellane. The charge density exhibits local maxima only at the positions of the nuclei, and as a consequence, all gradient paths in the neighborhood of a given nucleus terminate at the nucleus and define its basin. Saddle points exist between pairs of nuclei, and the positions of these bond critical points are denoted by black dots on the maps of the gradient vector fields. The two trajectories of $\nabla\rho$ that originate at each such point and terminate at the neighboring nuclei define the bond path, and they are shown in heavy line. Also shown in heavy line are two of the trajectories which terminate at each bond critical point and define the interatomic boundary separating neighboring atomic basins. The ring critical point in b is denoted by a triangle.

sidered to be bonded to one another is not restricted to inverted carbon atoms. It has been stated that such a result "seems to contradict the conventional view that a buildup of charge between the nuclei is necessary for covalent chemical bonding".[22]

The problem with such studies, both experimental and theoretical, lies in their use of an arbitrary reference state—superposed atom densities—to measure the extent of charge accumulation between a pair of nuclei. The properties of a quantum mechanical system are determined by its state function. Whether or not charge is accumulated between a pair of nuclei in a molecule—and an accumulation of charge is essential for the attainment of electrostatic equilibrium in the forces exerted on the nuclei—must be determined in an absolute manner and not with respect to an arbitrary and nonphysical reference density which can have no effect on the properties of the system under discussion. If a bond is to be a property of a system and if it is to provide a means for characterizing and summarizing the system's properties, then it should be determined by information contained in the state function. A method for characterizing the properties of a system in terms of the chemical concepts of atoms and bonds using only information contained in the electronic charge density as determined by the state function is described and illustrated in this and the following paper.[23]

In order to make meaningful comparisons of the properties of the atoms and bonds in molecules with usual and unusual structures we have examined a wide variety of saturated hydrocarbons: the alkanes **1–8**, the cycloalkanes **9–12**, the bicycloalkanes **13–19**, and the small ring propellanes **20–23**, as well as tetrahedrane (**24**), cubane (**25**), and spiropentane (**26**). In most cases the results are calculated from wave functions obtained by using the 6-31G* basis set at the corresponding optimized geometry,[6] calculations denoted as 6-31G*/6-31G*. In a few cases,

(5) Carlson, T. A. *Annu. Rev. Phys. Chem.* **1975**, *26*, 211. Wiberg, K. B.; Ellison, G. B.; Brundle, C. R.; Kuebler, N. A. *Chem. Phys. Lett.* **1976**, *41*, 37.

(6) Wiberg, K. B.; Wendoloski, J. J. *J. Am. Chem. Soc.* **1982**, *104*, 5679. Wiberg, K. B. *J. Am. Chem. Soc.* **1983**, *105*, 1227. Wiberg, K. B.; Bonneville, G.; Dempsey, R. *Isr. J. Chem.* **1983**, *23*, 85.

(7) (a) Wiberg, K. B.; Walker, F. H. *J. Am. Chem. Soc.* **1982**, *104*, 5239. (b) Wiberg, K. B.; Dailey, W. P.; Walker, F. H.; Waddell, S. T.; Crocker, L. S.; Newton, M. D. *J. Am. Chem. Soc.* **1985**, *107*, 7247.

(8) Stohrer, W. D.; Hoffmann, R. *J. Am. Chem. Soc.* **1972**, *94*, 779.

(9) Newton, M. D.; Schulman, J. M. *J. Am. Chem. Soc.* **1972**, *94*, 773.

(10) Jackson, J. E.; Allen, L. C. *J. Am. Chem. Soc.* **1984**, *106*, 591.

(11) Epiotis, N. D. *J. Am. Chem. Soc.* **1984**, *106*, 3170.

(12) Bader, R. F. W.; Cade, P. E.; Beddall, P. M. *J. Am. Chem. Soc.* **1971**, *93*, 3095.

(13) Wiberg, K. B.; Wendoloski, J. J. *J. Comput. Chem.* **1981**, *2*, 53.

(14) Streitwieser, A., Jr.; Grier, D. L.; Kohler, B. A. B.; Vorpagel, E. R.; Schriver, G. W. *Electron Distrib. Chem. Bond*, [*Proc. Symp.*] **1982**, 447.

(15) Francl, M. M.; Hout, R. R., Jr.; Hehre, W. J. *J. Am. Chem. Soc.* **1984**, *106*, 563.

(16) Coppens, P. *MTP Int. Rev. Sci.: Phys. Chem., Ser. Two* **1975**, *11*, 21.

(17) Dunitz, J. D. *X-ray Analysis and the Structure of Organic Molecules*; Cornell: Ithaca, NY, 1979; p 391ff.

(18) Stevens, E. D.; Rys, J.; Coppens, P. *J. Am. Chem. Soc.* **1978**, *100*, 2324. Stevens, E. D. *Acta Crystallogr., Sect. B: Struct. Crystallogr. Cryst. Chem.* **1980**, *B36*, 1870. Stevens, E. D.; Hope, H. *Acta Crystallogr., Sect. B: Struct. Crystallogr. Cryst. Chem.* **1977**, *A33*, 723.

(19) Benard, M.; Coppens, P.; Delucia, M. L.; Stevens, E. D. *Inorg. Chem.* **1980**, *19*, 1924.

(20) Breitenstein, M.; Dannöhl, H.; Meyer, H.; Schweig, A.; Zittlau, W. In *Electron Distributions and The Chemical Bond*; Coppens, P., Hall, M. B., Eds.; Plenum: New York, 1982.

(21) Chakrabarti, P.; Seiler, P.; Dunitz, J. D. *J. Am. Chem. Soc.* **1981**, *103*, 7378.

(22) Dunitz, J. D.; Seiler, P. *J. Am. Chem. Soc.* **1983**, *105*, 7056.

(23) Wiberg, K. B.; Bader, R. F. W.; Lau, C. D. H. *J. Am. Chem. Soc.*, in press.

namely, **11, 15, 17**, and **22**, the 6-31G* basis was used at the 4-31G optimized geometry, calculations denoted as 6-31G*/4-31G. The differences between the 4-31G and 6-31G* geometries are generally quite small.[3b] A partial comparison is also made between 6-31G**/6-31G* and 6-31G*/6-31G* results.

II. Atoms and Their Properties

Quantum mechanics defines an atom in a molecule. It does this by determining the properties of uniquely defined pieces of a molecule and yielding their equations of motion, equations that describe how these properties change with time.[24,25] This information suffices to define the physics of these pieces. The pieces themselves are unique because they must satisfy a particular condition determined by quantum mechanics. The condition is stated in terms of the paths traced out by the gradient vectors of the charge density. A gradient vector points in the direction of steepest ascent in the charge density. By following this direction starting from a given point, for a succession of closely spaced points, one can determine the path or trajectory traced out by a gradient vector of ρ. The collection of gradient paths associated with a charge distribution is called the gradient vector field, and the definition of atoms and structure is determined by the global properties of this field. Gradient vector fields of the charge density are illustrated in Figure 1.

The quantum condition defining the atom states that the atom shall be bounded by a surface that is not crossed by any trajectories of the gradient of ρ. This is referred to as the zero flux surface condition.[26] When applied to the gradient vector field associated with a molecular charge distribution, the zero flux surface condition leads to a partitioning of the space of the molecule into a set of nonoverlapping regions, each region containing a single nucleus. This partitioning of a molecule into atoms by the zero flux surface condition is a consequence of the dominant topological property exhibited by a charge distribution—that it exhibits local maxima only at the positions of the nuclei. As a consequence of this property, all of the trajectories in the neighborhood of a given nucleus terminate at that nucleus. Each nucleus acts as an *attractor* in the gradient vector field. The region of space traversed by all the paths that terminate at a given nucleus is called the *basin* of that attractor, and *an atom is defined as the union of an attractor and its basin*.[27-29] A review of this theory has appeared recently in *Accounts of Chemical Research*, and a fuller, qualitative description is given there.[30]

We are less concerned here with the quantum mechanical details of the theory than we are with the properties of the atoms it defines and their relationship to chemistry. The molecular structure hypothesis—that a molecule is a collection of atoms linked by a network of bonds—was forged in the crucible of 19th century experimental chemistry. It has evolved into the working hypothesis of chemistry as a consequence of the observation that atoms or groupings of atoms appear to exhibit characteristic sets of properties that can vary between relatively narrow limits. In certain situations the variation in properties is so slight that a group additivity scheme can be established. Thus the knowledge of chemistry is ordered, classified, and understood by assigning properties to atoms and functional groups and then relating the properties of the total system to those of its constituent atoms. The atoms defined by theory provide the physical basis for this hypothesis in the following way:[26] (1) They are the most

transferable pieces of a system that one can define in real space and, thus they maximize the transfer of information between molecules at the level of the charge density. (2) The average value of a property for the total system is obtained by summing the atomic averages for the same property over all the atoms in the molecule. (3) The most important characteristic of an atom is that the constancy in its properties, including its contribution to the total energy of a system, is observed to be directly determined by the constancy in its distribution of charge. When the distribution of charge over an atom is the same in two different molecules, i.e., when the atom or some functional grouping of atoms is the same in the real space of two systems, then it makes the same contribution to the total energy in both systems. It is because of the direct relationship between the spatial form of an atom and its properties that we are able to identify them in different systems.[26] This relationship has its basis in the observation that the atoms of this theory respond only to changes in the total force exerted on their charge distributions and not to changes in the individual contributions to this force, changes which are large even between closely related systems, be they members of a homologous series or chemically similar in structure. If it were not for this property of responding only to some net field (actually the virial of the total Ehrenfest force[25,26]) rather than to individual potential contributions, there would be no chemically recognizable atoms or functional groups.

The relationship between the form and the properties of an atom are most evident in the limit of an atom being transferable between systems without change. The resulting constancy in its properties, together with the fact that the value of a property for the total system is given by the sum of the atomic contributions (point 2 above), then leads to the existence of atomic or group additivity schemes. The most important and fundamental of these is additivity of the energy, and one of the earliest examples of this was observed for the homologous series of saturated hydrocarbons.[31] We demonstrate in the following paper[23] that the atoms defined by theory account for the additivity of the energy in this series of molecules and in doing so demonstrate that they are the chemical atoms. The present paper describes the bonds and the structures they define for molecules **1-26**, together with a discussion of the relative stabilities and reactivities of these structures. The following paper, in addition to accounting for energy additivity in terms of the properties of the individual atoms, particularly their energies and net charges, also uses the atomic properties to obtain an understanding of strain energy in the cyclic, bicyclic, and propellane molecules.

III. Bonds and Structure

The properties of a molecular charge distribution are summarized in terms of its critical points.[32a,b] These are points where the charge density is a maximum, a minimum, or a saddle, and at these points the gradient vector field of the charge density vanishes ($\nabla \rho = 0$). A critical point is characterized by the signs of its three principal curvatures of ρ. Thus at a maximum (minimum) in ρ, all three curvatures are negative (positive). A critical point with one positive curvature and two negative curvatures is found between every pair of neighboring nuclei (Figure 1). Such a critical point will be referred to as a *bond critical point*,[33] and the charge density has the appearance of a saddle when displayed in a plane containing the positive and one of the negative curvatures. The presence of such a critical point indicates that electronic charge is accumulated between the nuclei. This is a necessary condition for the existence of a bond,[34] and the definition is made quantitative through the definition of a bond path.[32a,33,35] Each of the two gradient paths that originate at the

(24) Srebrenik, S.; Bader, R. F. W. *J. Chem. Phys.* **1975**, *63*, 3945. Srebrenik, S.; Bader, R. F. W.; Nguyen-Dang, T. T. *J. Chem. Phys.* **1978**, *68*, 3667. Bader, R. F. W.; Srebrenik, S.; Nguyen-Dang, T. T. *J. Chem. Phys.* **1978**, *68*, 3680.

(25) Bader, R. F. W.; Nguyen-Dang, T. T. *Adv. Quantum Chem.* **1981**, *14*, 63.

(26) Bader, R. F. W.; Beddall, P. M. *J. Chem. Phys.* **1972**, *56*, 3320.

(27) Bader, R. F. W.; Anderson, S. G.; Duke, A. J. *J. Am. Chem. Soc.* **1979**, *101*, 1389.

(28) Bader, R. F. W.; Nguyen-Dang, T. T.; Tal, Y. *J. Chem. Phys.* **1979**, *70*, 4316.

(29) Bader, R. F. W.; Nguyen-Dang, T. T.; Tal, Y. *Rep. Prog. Phys.* **1981**, *44*, 893.

(30) Bader, R. F. W. *Acc. Chem. Res.* **1985**, *9*, 18.

(31) Franklin, J. L. *Ind. Eng. Chem.* **1949**, *41*, 1070.

(32) (a) Collard, K.; Hall, G. G. *Int. J. Quantum Chem.* **1977**, *12*, 623. (b) Smith, V. H.; Price, P. F.; Absar, I. *Isr. J. Chem.* **1977**, *16*, 187.

(33) Runtz, G.; Bader, R. F. W.; Messer, R. R. *Can. J. Chem.* **1977**, *55*, 3040.

(34) Bader, R. F. W.; Chandra, A. K. *Can. J. Chem.* **1968**, *46*, 953. Bader, R. F. W. *The Force Concept in Chemistry*; Deb, B. M., Ed.; Wiley: New York, 1980.

critical point and define the axis of the positive curvature terminate at one of the neighboring nuclei. They define a line linking the nuclei along which the charge density is a maximum with respect to any neighboring line. In an equilibrium geometry such a line is called a *bond path*, and its presence in such a case provides the necessary[34] and sufficient[36] conditions for the existence of a bond.

The network of bond paths defines a *molecular graph* and the structure of a molecule.[28,29] The structures determined in this manner for the molecules studied in this paper are shown in Figure 2. Each such network identifies the dominant set of interatomic interactions within a molecule as determined by the properties of its charge distribution. With the exception of the propellanes, these structures coincide with the traditional chemical bond structures assigned to these molecules assuming the directed electron pair model for the chemical bond, augmented with the concept of bent bonds. A bond path links the bridgehead nuclei in each of the propellane molecules **20–23**, even though this results in structures that have four bond paths, all to one side of a plane, terminating at each of the bridgehead nuclei for **20, 21,** and **22.** While the model of hybridized orbitals cannot describe such a situation, even assuming bent bonds, the results demonstrate that the charge distribution of a carbon atom can be so arranged as to yield bond paths which correspond to an inverted structure for the atom.

If the nuclei in a molecule are linked so as to form a ring, then a ring critical point is found in its interior. The charge density is a minimum at this point in the ring surface, Figure 1. If the nuclei are linked so as to enclose the interior of the molecule with ring surfaces as in **16**, for example, then another and final kind of critical point is found in the interior of the resulting cage structure. The charge density is a local minimum at such a cage critical point.

The structures of the propellanes consist of three rings, either three or four membered, sharing a common bond, the bridgehead bond. Addition of a molecule of hydrogen to a propellane breaks the bridgehead bond and yields a corresponding bicyclic molecule, **16–19.** Structures **16** and **19** are cage structures, the interior of each molecule being bounded by three curved ring surfaces and containing a cage critical point. Structure **18** is an open structure with two curved, five-membered ring surfaces with carbon 7 as a common apex[37] (Table I). Structure **17** possesses two ring critical points along the 2-fold symmetry axis: one defines a four-membered ring for carbons 1, 4, 5, and 6 while the other lies in the plane of carbons 1, 2, 3, and 4.[37]

The charge density is a minimum at the critical point along a bond path as the corresponding curvature of ρ, denoted by λ_3, is positive. It is a maximum at this same point in directions perpendicular to the bond path as the other two curvatures, λ_1 and λ_2, are negative. A set of trajectories of $\nabla\rho$ terminate at this two-dimensional maximum in ρ and define an interatomic surface. The trajectories associated with a bond critical point thus define both the bond path that links a pair of neighboring nuclei and the surface which separates their basins. While ρ has the appearance of a saddle in the region of a bond critical point when viewed in a plane containing the positive and one of the negative curvatures as in Figure 1, ρ is a maximum at this same point when viewed in the plane perpendicular to the bond path as defined by the two negative curvatures. Figure 3 illustrates such planes for the propellane molecules and their bicyclic congeners. In the propellanes, the planes shown are perpendicular to the bond path linking the bridgehead carbon nuclei at the bond critical point. Each plane exhibits a central maximum for the bridgehead bond, together with three nuclear maxima for each CH_2 group of a

(35) Bader, R. F. W. In *Physical Chemistry*; Buckingham, A. D., Coulson, C. A. Eds.; International Review of Science; Butterworths: London, 1975; Vol. 1.

(36) Bader, R. F. W.; Essen, H. *J. Chem. Phys.* **1984,** *80,* 1943.

(37) A decrease in the bridgehead bond angles 6-1-2 and 5-4-3 in **18** will result in the formation of a new critical point for the six-membered ring and transform this structure into a cage. The intersection of the gradient vectors associated with the two ring critical points in **17** is unstable.[29] An unsymmetrical motion of the carbon nuclei will change this structure into a cage or into an open structure similar to that for **18.**
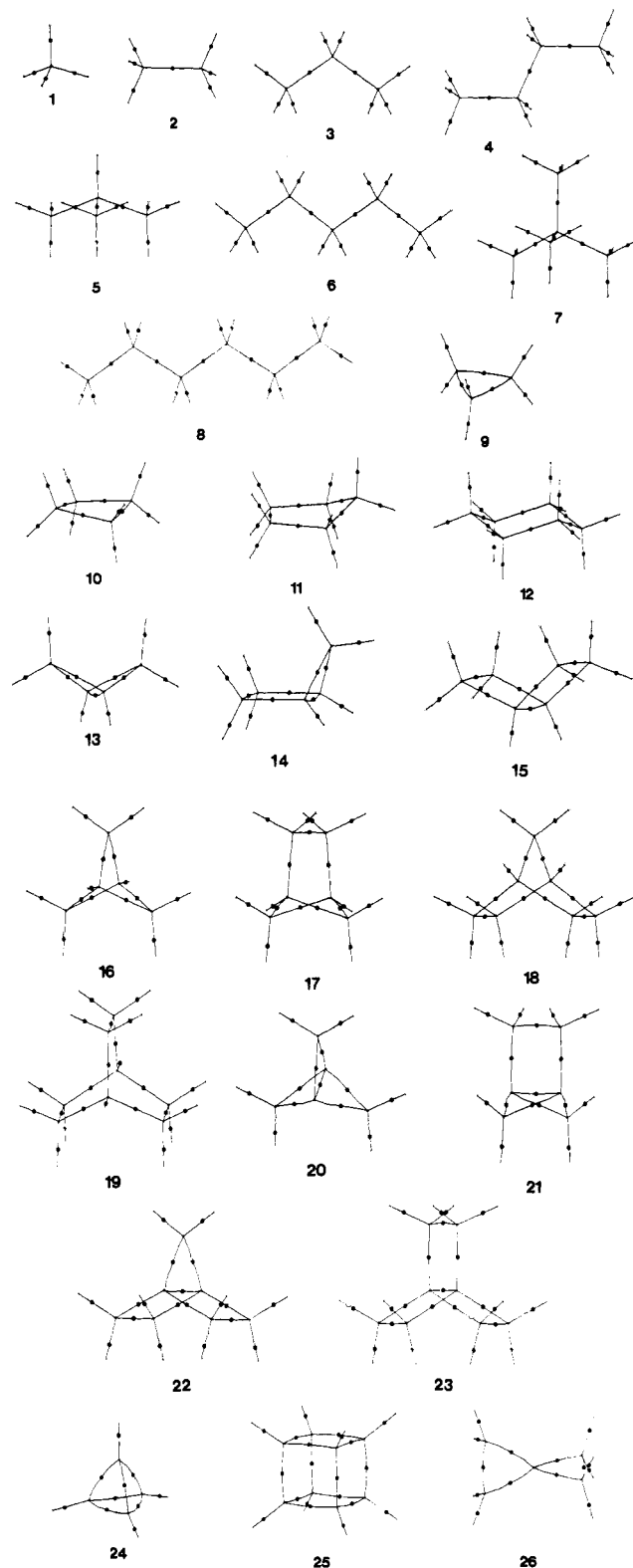

Figure 2. Planar projections of molecular graphs generated from the theoretical charge distributions. The bond critical points are denoted by black dots in these diagrams and also in Figures 4 and 5. Each structure is numbered according to Table I. The structures depicted in these diagrams are determined entirely by information contained in the electronic charge density.

three-membered ring and/or a maximum for the bond critical point of an outer bond in a four-membered ring. Thus the diagram for [2.2.2]propellane shows four local maxima corresponding to the presence of a central bridgehead bond and the three outer bonds of the four-membered rings, while the diagram for [1.1.1]propellane shows one central bond maximum and three
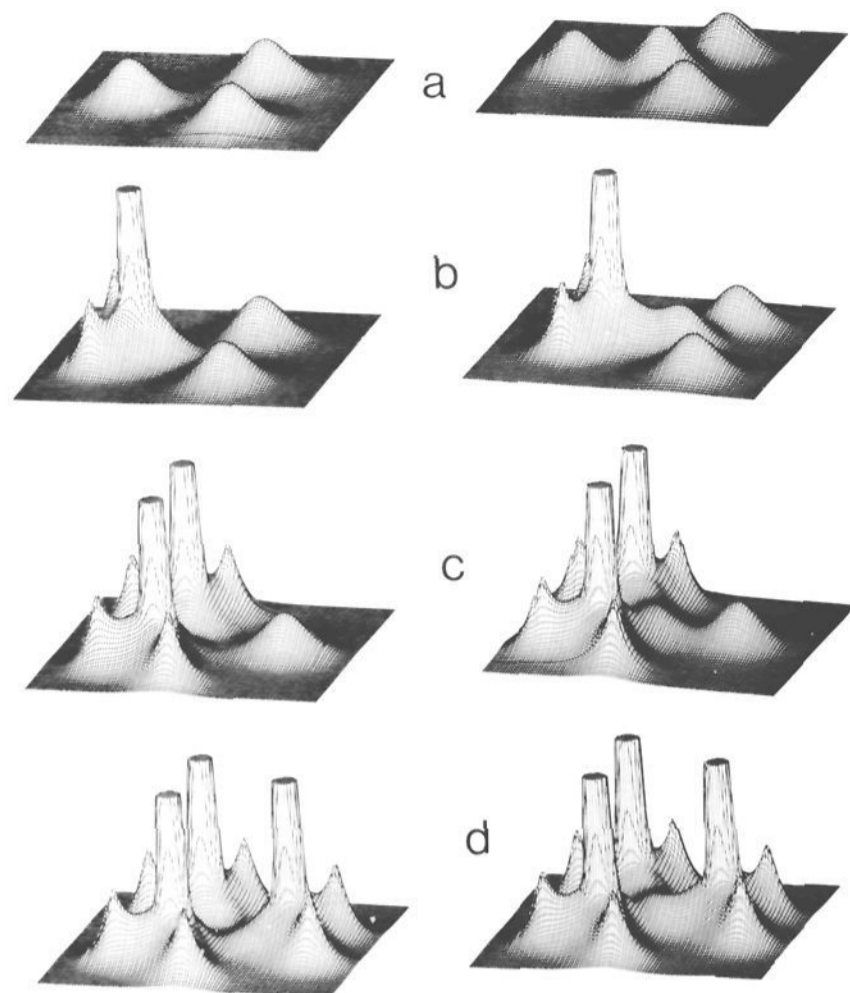
Figure 3. Relief maps of the charge density in the symmetry plane bisecting the bridgehead bond in the propellanes, shown on the right-hand side, and in the corresponding symmetry plane in each of the related bicyclic structures, shown on the left: (a) [2.2.2]propellane and bicyclooctane, (b) [2.2.1]propellane and norborane, (c) [2.1.1]propellane and bicyclohexane, (d) [1.1.1]propellane and bicyclopentane.

groupings of CH_2 nuclear maxima. The peripheral structure of ρ in the corresponding plane of the bicyclic molecules is similar, but in each case the central bond maximum is missing, as there is no line of maximum charge density linking their bridgehead nuclei. In **16** and **19** it is replaced by a local minimum corresponding to the presence of a cage critical point, in **17** it is replaced by the minimum in a ring surface, and in **18** the charge density decreases monotonically along the symmetry axis from the carbon nucleus forming the one-carbon bridge.

There is, therefore, an essential, qualitative difference in the manner in which electronic charge is distributed along a line linking a pair of bonded nuclei (as between the bridgehead nuclei in the propellanes) and along a line linking two nuclei that are not bonded (as between the bridgehead nuclei in the corresponding bicyclic structures). It has been stated by Newton and Schulman[9] and quoted by Jackson and Allen[10] "that the electron density in the interbridgehead region (of [1.1.1]propellane) is little different from that in bicyclo[1.1.1]pentane, a compound in which no formal bridgehead–bridgehead bond exists." This statement is at variance with the above findings. Qualitatively, the two charge distributions differ in form, the former exhibiting a charge maximum in the internuclear plane, the latter a minimum. Quantitatively, the value of ρ at the bond critical point in the propellane molecule, 0.203 au, is four-fifths the value of that for a normal C–C single bond, while the value of ρ at the corresponding cage point in the bicyclic molecule is 0.098 au. It is also clear from Figure 3 that the values of ρ at the bond critical point and the three adjacent ring critical points in [1.1.1]propellane are almost equal, giving rise to a very broad bonded maximum in ρ in the interatomic surface (the two negative curvatures of ρ are small in magnitude for the bond critical point, Table I). Hence there is an appreciable accumulation of charge between the bridgehead nuclei in this molecule, greater than that suggested on the basis of the value of ρ at the bond critical point alone. Indeed, the bridgehead bond could well be designated a "fat bond", as the C–C interatomic surface in this plane is the triangular face formed by the three ring critical points, and electronic charge is accumulated to a nearly constant extent

over the whole of this surface, as opposed to decaying rapidly from its maximum value at the bond critical point as it does for a regular C–C bond (compare with an outer bonded maximum in Figure 3).

A recent analysis[7b] of the infrared spectrum of [1.1.1]propellane has shown that the bridgehead internuclear separation is 0.05 Å longer than that reported here for the 6-31G* basis. The experimental result is in agreement with a theoretical calculation which includes electron correlation.[7b] The same calculation predicts the corresponding triplet diradical to lie about 74 kcal mol^{-1} above the ground state and to possess a bridgehead separation larger by 0.22 Å. This result is in line with a previous estimate of Wiberg[6] that 65 kcal/mol are required to rupture the bridgehead bond in [1.1.1]propellane to obtain the corresponding diradical. These observations are interpreted[7b] to imply that the bridgehead carbons are "bonded". They are understandable if there is an accumulation of electronic charge between the bridgehead nuclei in the ground state of [1.1.1]propellane as is indeed the case.

The fundamental difference in the manner in which electronic charge is distributed in the bridgehead internuclear region, between the propellanes and the corresponding bicyclic molecules, is not made apparent in density difference maps. Such deformation maps show a region of charge depletion between these nuclei for the propellanes as well as for the bicyclic molecules.[10,21] First, there is no physical basis for demanding that a density difference map in a polyatomic molecule show a charge buildup between a pair of nuclei if the nuclei are to be considered bonded to one another.[38] Second, the reference density, in addition to being physically nonrealizable, is arbitrary in its construction. Different results are obtained and different conclusions are reached depending on whether one employs spherical atom densities or densities of atoms in prepared valence states in the construction of the promolecule density.[34,39,40] Third, in performing a comparison between density difference maps for pairs of molecules, as Jackson and Allen[10] do for [1.1.1]propellane and various cyclic and bicyclic molecules, one is actually comparing four different charge distributions. It is clear that the spherical atom promolecule density for bicyclo-[1.1.1]pentane will, because of the larger bridgehead separation of 1.87 Å, subtract considerably less charge from the bridgehead symmetry plane than will the corresponding promolecule density for the equilibrium geometry of [1.1.1]propellane where the corresponding separation is calculated to be 1.54 Å. Thus their observation of an "essential similarity"[10] in the deformation density distributions for these two molecules, in particular the lack of a charge buildup between the bridgehead nuclei, is an artifact of the promolecule distributions and is not a reflection of the relative properties of the two charge distributions of interest. Qualitatively and of fundamental importance, the propellane molecule does accumulate charge at the bond midpoint and along the resultant bond path, while the bicyclic compound exhibits a local minimum in ρ in this same region. In addition, as demonstrated by a direct quantitative comparison of their charge distributions, the bicyclic molecule has significantly less charge in this region than does the propellane molecule. These essential observations are lost in a comparison of the deformation densities because the reference density for propellane removes more charge from the critical bridgehead region than does that for the bicyclic molecule. Why complicate a comparison of two distributions through the introduction of two more distributions which are arbitrary in their definition and are of no direct physical interest?

(38) A simple electrostatic argument based on Gauss' theorem shows that a promolecule density for a diatomic molecule composed of spherical atom densities does not place sufficient charge in the binding region to balance the forces of nuclear repulsion. Thus for a diatomic molecule, but not for a polyatomic one, a necessary condition for electrostatic equilibrium is that the deformation density exhibit a charge accumulation in the binding region. Cf.: Bader, R. F. W. *An Introduction to the Electronic Structure of Atoms and Molecules*; Clark, Irwin: Toronto, 1970.

(39) Bader, R. F. W.; Henneker, W. H.; Cade, P. E. *J. Chem. Phys.* **1967**, *46*, 3341.

(40) Ransil, B. J.; Sinai, J. J. *J. Chem. Phys.* **1967**, *46*, 4050. Kunze, K. L.; Hall, M. B. *J. Am. Chem. Soc.* **1986**, *108*, 5122.

Table I. Bond Properties in Hydrocarbons 6-31G*/6-31G*

formula	structure	bond	R_c, Å	R_b, Å	r_A, Å	r_B, Å	n	ρ_b, e/a_o^3	$\nabla^2\rho_b$, e/a_o^5	λ_1, e/a_o^5	λ_2, e/a_o^5	λ_3, e/a_o^5	ϵ	ρ_r and ρ_c, e/a_o^3
					a. Acyclic Compounds									
CH_4, **1**		C–H	1.0836		0.6814	0.4022		0.2772	−0.9801	−0.7185	−0.7185	0.4569	0.0000	
C_2H_6, **2**		C–C	1.5274		0.7637	0.7637	1.00	0.2520	−0.6604	−0.4766	−0.4766	0.2928	0.0000	
		C–H	1.0856		0.6808	0.4048		0.2787	−0.9838	−0.7250	−0.7182	0.4595	0.0095	
C_3H_8, **3**		C–C	1.5283		0.7677	0.7606	1.01	0.2540	−0.6868	−0.4845	−0.4798	0.2957	0.0098	
		C1–H4	1.0858		0.6806	0.4051		0.2784	−0.9824	−0.7231	−0.7170	0.4576	0.0085	
		C1–H5	1.0866		0.6808	0.4058		0.2777	−0.9754	−0.7195	−0.7139	0.4580	0.0078	
		C2–H	1.0873		0.6806	0.4068		0.2800	−0.9886	−0.7282	−0.7222	0.4617	0.0083	
n-C_4H_{10}, **4**		C1–C2	1.5277		0.7673	0.7605	1.01	0.2541	−0.6694	−0.4842	−0.4803	0.2951	0.0082	
		C2–C3	1.5302		0.7651	0.7651	1.02	0.2555	−0.6735	−0.4906	−0.4813	0.2985	0.0192	
		C1–H5	1.0847		0.6798	0.4049		0.2790	−0.9867	−0.7250	−0.7188	0.4571	0.0086	
		C1–H6	1.0858		0.6802	0.4057		0.2782	−0.9787	−0.7211	−0.7155	0.4579	0.0079	
		C2–H	1.0880		0.6803	0.4077		0.2792	−0.9813	−0.7232	−0.7181	0.4600	0.0070	
i-C_4H_{10}, **5**		C–C	1.5302		0.7707	0.7595	1.02	0.2551	−0.6727	−0.4873	−0.4831	0.2976	0.0086	
		C1–H5	1.0874		0.6809	0.4065		0.2769	−0.9682	−0.7149	−0.7104	0.4571	0.0062	
		C1–H6	1.0861		0.6803	0.4058		0.2781	−0.9788	−0.7203	−0.7150	0.4565	0.0075	
		C2–H	1.0884		0.6804	0.4080		0.2813	−0.9945	−0.7289	−0.7289	0.4634	0.0000	
n-C_5H_{12}, **6**		C1–C2	1.5269		0.7666	0.7603	1.02	0.2546	−0.6714	−0.4853	−0.4815	0.2953	0.0079	
		C2–C3	1.5281		0.7638	0.7642	1.03	0.2565	−0.6786	−0.4926	−0.4843	0.2983	0.0017	
		C1–H6	1.0848		0.6799	0.4049		0.2789	−0.9870	−0.7250	−0.7191	0.4572	0.0082	
		C1–H7	1.0863		0.6806	0.4058		0.2779	−0.9769	−0.7201	−0.7148	0.4581	0.0074	
		C2–H	1.0885		0.6806	0.4079		0.2790	−0.9793	−0.7220	−0.7174	0.4600	0.0064	
		C3–H	1.0895		0.6806	0.4090		0.2780	−0.9703	−0.7160	−0.7125	0.4582	0.0049	
neo-C_5H_{12}, **7**		C–C	1.5332		0.7732	0.7601	1.02	0.2552	−0.6719	−0.4853	−0.4853	0.2987	0.0000	
		C–H	1.0866		0.6803	0.4063		0.2778	−0.9752	−0.7178	−0.7131	0.4559	0.0066	
n-C_6H_{14}, **8**		C1–C2	1.5284		0.7677	0.7606	1.01	0.2538	−0.6678	−0.4834	−0.4794	0.2950	0.0083	
		C2–C3	1.5298		0.7648	0.7650	1.02	0.2554	−0.6736	−0.4900	−0.4815	0.2979	0.0176	
		C3–C4	1.5296		0.7648	0.7648	1.02	0.2554	−0.6738	−0.4894	−0.4817	0.2973	0.0160	
		C1–H7	1.0857		0.6805	0.4052		0.2784	−0.9823	−0.7229	−0.7168	0.4574	0.0086	
		C1–H8	1.0864		0.6807	0.4058		0.2778	−0.9761	−0.7199	−0.7142	0.4580	0.0079	
		C2–H	1.0880		0.6803	0.4077		0.2793	−0.9818	−0.7234	−0.7185	0.4601	0.0069	
		C3–H	1.0889		0.6803	0.4087		0.2784	−0.9737	−0.7180	−0.7141	0.4584	0.0054	
					b. Cyclic Compounds									
C_3H_6, **9**		C–C	1.4974	1.5069	0.7511	0.7511	0.98	0.2490	−0.5331	−0.4892	−0.3284	0.2846	0.4896	$\rho_r = 0.2044$
		C–H	1.0759		0.6802	0.3958		0.2849	−1.0383	−0.7604	−0.7412	0.4632	0.0260	
C_4H_8, **10**		C–C	1.5485	1.5507	0.7751	0.7751	0.97	0.2467	−0.6269	−0.4616	−0.4610	0.2958	0.0014	$\rho_r = 0.0847$
		C1–H5	1.0848		0.6818	0.4030		0.2806	−1.0034	−0.7355	−0.7312	0.4633	0.0059	
		C1–H9	1.0848		0.6815	0.4034		0.2796	−0.9922	−0.7303	−0.7243	0.4624	0.0082	
C_5H_{10}, **11**^{a}		C1–C2	1.5377		0.7688	0.7689	1.00	0.2517	−0.6504	−0.4755	−0.4730	0.2981	0.0053	$\rho_r = 0.0359$
		C2–C3	1.5449		0.7722	0.7728	0.97	0.2482	−0.6349	−0.4672	−0.4643	0.2966	0.0063	
		C3–C4	1.5515		0.7758	0.7758	0.96	0.2451	−0.6212	−0.4596	−0.4567	0.2952	0.0064	
		C1–H6	1.0836		0.6783	0.4053		0.2813	−1.0020	−0.7314	−0.7281	0.4575	0.0046	
		C1–H7	1.0841		0.6772	0.4070		0.2812	−0.9964	−0.7299	−0.7240	0.4575	0.0081	
		C2–H8	1.0839		0.6772	0.4067		0.2816	−0.9989	−0.7320	−0.7250	0.4581	0.0096	
		C2–H9	1.0826		0.6776	0.4050		0.2820	−1.0068	−0.7343	−0.7299	0.4575	0.0061	
		C3–H10	1.0832		0.6779	0.4053		0.2820	−1.0043	−0.7348	−0.7282	0.4587	0.0090	
		C3–H11	1.0838		0.6778	0.4059		0.2819	−1.0010	−0.7341	−0.7261	0.4592	0.0109	
C_6H_{12}, **12**		C–C	1.5325		0.7663	0.7663	1.02	0.2543	−0.6673	−0.4837	−0.4807	0.2971	0.0062	$\rho_r = 0.0176$
		C1–H7	1.0870		0.6799	0.4071		0.2798	−0.9882	−0.7248	−0.7210	0.4576	0.0053	
		C1–H8	1.0892		0.6803	0.4090		0.2780	−0.9700	−0.7161	−0.7121	0.4582	0.0057	

c. Bicyclic Compounds

Compound	Bond													
C$_4$H$_6$, **13**	C1–C3	1.4658	1.4819	0.7376	0.7376	0.98	0.2488	−0.3791	−0.3890	−0.2692	0.2792	0.4450	ρ_r = 0.2120
	C1–C2	1.4886	1.4966	0.7538	0.7384	1.01	0.2541	−0.5341	−0.4944	−0.3232	0.2836	0.5295	
	C1–H5	1.0697		0.6841	0.3856		0.2854	−1.0630	−0.7756	−0.7485	0.4611	0.0362	
	C2–H6	1.0781		0.6826	0.3956		0.2854	−1.0485	−0.7682	−0.7480	0.4678	0.0270	
	C2–H7	1.0832		0.6855	0.3977		0.2828	−1.0210	−0.7534	−0.7396	0.4719	0.0187	
C$_5$H$_8$, **14**	C1–C4	1.5129	1.5261	0.7602	0.7602	0.95	0.2440	−0.4877	−0.4748	−0.3059	0.2930	0.5523	$\rho_r(3)$ = 0.2063
	C1–C2	1.5282	1.5304	0.7757	0.7542	1.02	0.2559	−0.6668	−0.4935	−0.4746	0.3012	0.0399	
	C1–C5	1.4935	1.5033	0.7496	0.7485	1.00	0.2528	−0.5472	−0.4973	−0.3348	0.2849	0.4856	
	C2–C3	1.5578	1.5601	0.7798	0.7798	0.94	0.2425	−0.6100	−0.4600	−0.4478	0.2979	0.0273	
	C1–H6	1.0753		0.6812	0.3941		0.2849	−1.0451	−0.7656	−0.7421	0.4626	0.0317	$\rho_r(4)$ = 0.0872
	C3–H9	1.0834		0.6809	0.4025		0.2819	−1.0094	−0.7368	−0.7349	0.4623	0.0026	
	C3–H10	1.0856		0.6821	0.4036		0.2805	−0.9984	−0.7352	−0.7282	0.4649	0.0096	
	C5–H12	1.0768		0.6806	0.3962		0.2842	−1.0341	−0.7594	−0.7360	0.4614	0.0318	
	C5–H13	1.0795		0.6814	0.3980		0.2833	−1.0162	−0.7480	−0.7312	0.4629	0.0229	
C$_6$H$_{10}$, **15**^{a}	C1–C4	1.5734	1.5985	0.7888	0.7888	0.92	0.2398	−0.5893	−0.4489	−0.4443	0.3040	0.0103	
	C1–C2	1.5493	1.5629	0.7761	0.7749	0.97	0.2479	−0.6326	−0.4687	−0.4645	0.3006	0.0091	ρ_r = 0.0816
	C1–C6	1.5524	1.5545	0.7775	0.7766	0.96	0.2466	−0.6262	−0.4654	−0.4606	0.2998	0.0104	
	C2–C3	1.5600		0.7807	0.7811	0.94	0.2418	−0.6070	−0.4546	−0.4486	0.2962	0.0133	
	C1–H7	1.0782		0.6763	0.4014		0.2851	−1.0376	−0.7492	−0.7481	0.4597	0.0015	
	C2–H8	1.0817		0.6782	0.4035		0.2822	−1.0097	−0.7368	−0.7320	0.4592	0.0066	
	C2–H9	1.0817		0.6779	0.4038		0.2821	−1.0088	−0.7380	−0.7310	0.4602	0.0095	
	C3–H10	1.0814		0.6781	0.4033		0.2824	−1.0116	−0.7382	−0.7326	0.4592	0.0077	
	C3–H11	1.0818		0.6781	0.4037		0.2820	−1.0073	−0.7373	−0.7302	0.4602	0.0097	
C$_5$H$_8$, **16**	C–C	1.5457	1.5507	0.7740	0.7757	0.96	0.2457	−0.5984	−0.4502	−0.4499	0.3017	0.0007	ρ_r = 0.1020
	C1–H6	1.0823		0.6839	0.3984		0.2826	−1.0337	−0.7511	−0.7511	0.4685	0.0000	
	C2–H7	1.0846		0.6812	0.4034		0.2819	−1.0111	−0.7404	−0.7323	0.4616	0.0111	ρ_c = 0.0983
C$_6$H$_{10}$, **17**^{a}	C1–C5	1.5583	1.5615	0.7772	0.7837	0.94	0.2421	−0.5919	−0.4460	−0.4442	0.2982	0.0041	
	C1–C2	1.5418	1.5421	0.7741	0.7679	1.00	0.2517	−0.6444	−0.4760	−0.4677	0.2994	0.0178	ρ_r = 0.0468
	C2–C3	1.5639	1.5641	0.7821	0.7821	0.92	0.2397	−0.5933	−0.4470	−0.4392	0.2929	0.0178	
	C1–H7	1.0770		0.6775	0.3995		0.2865	−1.0566	−0.7597	−0.7574	0.4605	0.0031	$\rho_r(1,1)$ = 0.0916
	C2–H8	1.0822		0.6777	0.4045		0.2827	−1.0120	−0.7366	−0.7337	0.4583	0.0039	
	C5–H13	1.0816		0.6772	0.4044		0.2826	−1.0161	−0.7369	−0.7364	0.4571	0.0007	
	C5–H14	1.0807		0.6777	0.4045		0.2827	−1.0120	−0.7366	−0.7337	0.4583	0.0039	
C$_7$H$_{12}$, **18**	C1–C7	1.5392	1.5399	0.7656	0.7741	1.00	0.2525	−0.6454	−0.4737	−0.4719	0.3001	0.0038	$\rho_r(5)$ = 0.0418
	C1–C2	1.5425	1.5427	0.7691	0.7735	1.00	0.2517	−0.6481	−0.4753	−0.4718	0.2990	0.0074	
	C2–C3	1.5577	1.5578	0.7789	0.7789	0.94	0.2424	−0.6071	−0.4524	−0.4478	0.2930	0.0103	
	C1–H	1.0853		0.6809	0.4044		0.2815	−1.0080	−0.7336	−0.7326	0.4582	0.0015	
	C7–H	1.0869		0.6801	0.4068		0.2789	−0.9839	−0.7202	−0.7180	0.4543	0.0030	
	C2–H9	1.0856		0.6793	0.4063		0.2806	−0.9930	−0.7278	−0.7233	0.4580	0.0062	
	C2–H10	1.0853		0.6794	0.4059		0.2806	−0.9931	−0.7278	−0.7236	0.4582	0.0058	
C$_8$H$_{14}$, **19**	C1–C2	1.5352	1.5353	0.7639	0.7714	1.02	0.2550	−0.6672	−0.4839	−0.4820	0.2986	0.0039	ρ_r = 0.0216
	C2–C3	1.5510	1.5511	0.7755	0.7755	0.96	0.2450	−0.6236	−0.4580	−0.4576	0.2921	0.0008	
	C1–H	1.0855		0.6779	0.4076		0.2824	−1.0052	−0.7310	−0.7310	0.4569	0.0000	ρ_c = 0.0211
	C2–H	1.0857		0.6783	0.4074		0.2806	−0.9900	−0.7264	−0.7205	0.4569	0.0082	

d. Propellanes and Others

Compound	Bond													
C$_5$H$_6$, **20**	C1–C3	1.5430		0.7715	0.7715	0.73	0.2030	+0.0253	−0.1089	−0.1089	0.2432	0.0000	ρ_r = 0.1990
	C1–C2	1.5020	1.5112	0.7398	0.7632	1.00	0.2515	−0.5248	−0.4914	−0.3176	0.2843	0.5472	
	C2–H	1.0750		0.6862	0.3888		0.2898	−1.0924	−0.7864	−0.7799	0.4739	0.0084	
C$_6$H$_8$, **21**	C1–C4	1.5944	1.5955	0.7976	0.7976	0.70	0.1971	−0.0674	−0.2820	−0.0347	0.2493	7.1237	$\rho_r(3)$ = 0.1961
	C1–C2	1.5468	1.5483	0.7956	0.7522	0.96	0.2461	−0.6216	−0.4666	−0.4488	0.2938	0.0396	
	C1–C5	1.4926	1.5022	0.7382	0.7558	1.01	0.2530	−0.5355	−0.4975	−0.3176	0.2796	0.5664	
	C2–C3	1.5387	1.5413	0.7704	0.7704	1.00	0.2526	−0.6555	−0.4813	−0.4747	0.3006	0.0140	
	C2–H7	1.0820		0.6819	0.4001		0.2833	−1.0217	−0.7477	−0.7396	0.4656	0.0109	$\rho_r(4)$ = 0.0883
	C5–H12	1.0781		0.6877	0.3904		0.2874	−1.0685	−0.7747	−0.7690	0.4751	0.0075	
	C5–H11	1.0775		0.6857	0.3918		0.2868	−1.0661	−0.7716	−0.7665	0.4721	0.0067	

Table I (Continued)

formula	structure	bond	R_e, Å	R_b, Å	r_A, Å	r_B, Å	n	ρ_b e/a_0^3	$\nabla^2\rho_b$ e/a_0^5	λ_1 e/a_0^5	λ_2 e/a_0^5	λ_3 e/a_0^5	ϵ	ρ_r and ρ_c e/a_0^3
C_7H_{10}, **22**a		C1-C4	1.5343	1.5388	0.7673	0.7673	0.98	0.2482	-0.4922	-0.4914	-0.3013	0.3005	0.6312	$\rho_r(3) = 0.2130$
		C1-C2	1.5452	1.5482	0.7874	0.7600	0.95	0.2438	-0.6033	-0.4625	-0.4344	0.2936	0.0647	
		C1-C7	1.4973	1.5049	0.7490	0.7508	0.97	0.2477	-0.4959	-0.4887	-0.2816	0.2744	0.7355	
		C2-C3	1.5808	1.5832	0.7914	0.7914	0.89	0.2341	-0.5720	-0.4376	-0.4283	0.2939	0.0217	
		C2-H8	1.0819		0.6811	0.4008		0.2834	-1.0234	-0.7505	-0.7387	0.4658	0.0161	$\rho_r(4) = 0.0869$
		C2-H9	1.0804		0.6802	0.4003		0.2836	-1.0253	-0.7473	-0.7410	0.4630	0.0085	
		C7-H	1.0714		0.6798	0.3916		0.2887	-1.0749	-0.7762	-0.7636	0.4648	0.0165	
C_8H_{12}, **23**		C1-C4	1.5122		0.7561	0.7561	1.26	0.2878	-0.8303	-0.5821	-0.5821	0.3339	0.0000	$\rho_r = 0.0861$
		C1-C2	1.5508	1.5545	0.7760	0.7758	0.95	0.2441	-0.6083	-0.4615	-0.4458	0.2978	0.0381	
		C2-C3	1.5745	1.5768	0.7883	0.7883	0.90	0.2360	-0.5810	-0.4393	-0.4353	0.2936	0.0090	
		C-H	1.0859		0.6825	0.4034		0.2795	-0.9899	-0.7308	-0.7215	0.4624	0.0129	
C_4H_4, **24**		C-C	1.4634	1.4842	0.7378	0.7378	1.02	0.2551	-0.4672	-0.3813	-0.3733	0.2874	0.0213	$\rho_r = 0.2013$
		C-H	1.0635		0.6890	0.3745		0.2852	-1.0965	-0.7747	-0.7747	0.4528	0.0000	$\rho_c = 0.1833$
C_8H_8, **25**		C-C	1.5632	1.5677	0.7834	0.7834	0.95	0.2440	-0.6079	-0.4571	-0.4546	0.3038	0.0057	$\rho_r = 0.0814$
		C-H	1.0852		0.6858	0.3994		0.2786	-0.9989	-0.7307	-0.7307	0.4635	0.0000	$\rho_c = 0.0118$
C_5H_8, **26**		C1-C2	1.5127	1.5213	0.7586	0.7586	0.94	0.2425	-0.5005	-0.4722	-0.3138	0.2855	0.5049	$\rho_r = 0.2036$
		C1-C3	1.4789	1.4923	0.7369	0.7491	1.03	0.2571	-0.5719	-0.5027	-0.3623	0.2931	0.3874	
		C-H	1.0772		0.6817	0.3955		0.2839	-1.0322	-0.7578	-0.7394	0.4650	0.0249	

a The data for these structures are from a 6-31G*/4-31G calculation.

Jackson and Allen[10] ascribe the bonding between the bridgehead carbon atoms in [1.1.1]propellane to a particular degenerate pair of orbitals which concentrate their density off the bridgehead axis and coin the term "σ-bridged-π" to describe the bond. They consider only a subset of the orbitals in their analysis. The HOMO of [1.1.1]propellane is the in-phase overlap of $2p\sigma$ orbitals on the bridgehead carbons. A plot of an outer envelope of this orbital shows it to be spatially more diffuse in the antibinding than in the binding regions. Jackson and Allen claim this orbital is nonbonding or slightly antibonding and that it puts very little charge density between the bridgehead nuclei and "contributes nil to holding C_1 to C_3". This orbital is bonding as determined by the criteria set forth by Mulliken.[41,42] It has long been recognized that a molecular orbital formed by the in-phase overlap of $2p\sigma$ orbitals concentrates charge density in both the binding and antibinding regions with respect to the nuclei.[39,43] A comparison with the outer contour for the corresponding $3\sigma_g$ orbital for homonuclear diatomics, O_2, for example,[39] shows that the latter is also extreme in its differing spatial extents in the antibinding over the binding region. While classed as only weakly bonding or binding, this orbital in O_2 does exert a small net force drawing the nuclei together,[39] the reason being that the charge density is more contracted along the internuclear axis in the binding region than it is in the antibinding regions. Thus the relative size of an outer contour in different spatial regions provides no quantitative indication of the total amount of charge accumulated in the regions or of the relative strengths of the forces their densities exert on the nuclei.[39,43] The HOMO in fact contributes approximately one-third to the total density between the bridgehead nuclei in [1.1.1]propellane. Nor can one ignore contributions from other orbitals to the density in a particular region of space, contributions which even out the extremes present in any single orbital. The principal contribution to the bonding density between all second-row atoms comes from the overlap of 2s orbitals ($2\sigma_g$ in homonuclear diatomics), and the same is true in propellane. It is not possible to determine the extent of charge accumulation between a pair of nuclei by considering the properties of a single molecular orbital, and Jackson and Allen mistakenly conclude that there is "very little charge density along the C_1–C_3 line of centers" and ascribe the bonding to charge accumulations from a degenerate pair of off-axis orbitals. In terms of the properties of the *total* charge density, there is a line linking the bridgehead nuclei along which the density is a *maximum with respect to all neighboring lines*. Jackson and Allen state that the same σ-bridged-π bonding exists to a lesser extent in the corresponding [1.1.1]bicyclic compound which does not possess a bridgehead bond. As detailed above, the total charge distributions in the bridgehead regions of these two molecules differ in both form and extent.

The discussion so far has emphasized the possibility of determining whether or not two atoms are bonded to one another by using properties of the total charge density. This has established that the bridgehead nuclei in the propellanes are bonded to one another—that the distribution of charge between them has the same qualitative property of exhibiting a line of maximum charge accumulation linking the nuclei as is found between bonded nuclei in hydrocarbon molecules with more usual structures (Figure 2). While the bridgehead bonds exist, they differ in important respects from a normal C–C single bond, and they differ in ways that affect both the stability and reactivity of the propellane molecules. The classification of bonds and the characterization of their stabilities and reactivities are discussed in the following section.

IV. Properties of Bonds in Saturated Hydrocarbons

Bond Order. Bonds can be characterized in terms of properties of the bond path and of ρ at the bond critical point. These properties are given in Table I. The value of the charge density at a C–C bond critical point, the quantity ρ_b, may be fitted to yield an expression for a *bond order* n.[44] For densities obtained

(41) Mulliken, R. S. *Rev. Mod. Phys.* **1932**, *4*, 1.
(42) Mulliken, R. S. *Phys. Rev.* **1939**, *56*, 778.
(43) Bader, R. F. W. *Can. J. Chem.* **1963**, *41*, 2303.

by using the 6-31G* basis, n is given by

$$n = \exp\{6.458(\rho_b - 0.2520)\}$$

This definition yields values of 1.00, 1.62, 2.05, and 2.92 for the C-C bond orders in ethane, benzene, ethylene, and acetylene, respectively. This empirical bond order is only meant to provide a convenient measure of the extent to which electronic charge is accumulated between pairs of bonded nuclei relative to a set of standard values. In the acyclic hydrocarbons, interior bonds and bonds in the branched structures have the highest bond orders, with $n = 1.02-1.03$. Bond orders slightly less than unity are found for C-C bonds in the cyclic and bicyclic molecules. The smallest values are found for the bridgehead bonds in [1.1.1]- and [2.1.1]propellanes. As noted previously,[6] the bridgehead bond in [2.2.2]propellane has a relatively high value for ρ_b, yielding an order of 1.3. Bond orders are not simply correlated with bond length, and a smaller R_e does not necessarily imply a greater accumulation of charge along the bond path. For example, a C-C bond is longer in a branched alkane than in ethane, but its order is greater. The ring bonds of cyclopropane and certain of those in the three-membered rings of **13** and **14** are considerably shorter than the C-C bond in ethane but are of unit order. The [2.1.1]- and [2.2.1]propellanes also have three-membered-ring bonds with R_e values less than 1.50 Å, and in these very strained molecules the bond orders are less than unity.

While the values of ρ_b for the C-H bonds exhibit a much smaller variation—they are all formally of order 1—there are important trends. In the acyclic alkanes the value of ρ_b increases in the order $CH_4 < CH_3 < CH_2 < CH$. The value of ρ_b is greater still for the C-H bond in cyclopropane and decreases in value as the ring size increases, exhibiting the acyclic value in cyclohexane. Still larger values are found for the C-H bonds in the more strained bicyclic structures, particularly for hydrogens bonded to bridgehead carbons. The largest values of all are found for the C-H bonds of the three-membered rings of the propellanes. The trend in the values of ρ_b parallels the increase in the percent s character of the C-H bond as discussed in the following paper.[23] A C-H bond in cyclopropane has a greater percent s character, a shorter bond length, a larger stretch frequency, and a larger dissociation energy than any C-H bond in an acyclic alkane, in agreement with the larger value of ρ_b in the cyclic molecule. The decrease in ρ_b with ring size to the values found in cyclopentane and cyclohexane correlates with corresponding decreases in percent s character, C-H stretch frequency, and bond dissociation energy.[45a] For cyclohexane itself, ρ_b is greater for equatorial than for axial hydrogen and, again, the C-H frequency and dissociation energy exhibit identical trends.

Bond Path Angle and Length. The bond paths are noticeably curved in those structures where the geometry of the molecule precludes the possibility of tetrahedrally directed bonds between carbon nuclei.[33] The *bond path angle* α_b, the limiting value of the angle subtended at a nucleus by two bond paths, when compared to the corresponding geometrical or so-called bond angle α_e, is important in quantifying the concept of bond strain in these structures.[46a] Another related quantity is the *bond path length*, R_b, which for a curved bond path exceeds the corresponding internuclear separation or so-called bond length, R_e.[47] The C-H bond paths do not exhibit any significant curvature.

Values of the bond path angle and the difference $\Delta\alpha = \alpha_b - \alpha_e$ are listed in Table II for the cyclic, bicyclic, and propellane molecules together with their strain energies[46a] as calculated with Franklin's group equivalents. For most molecules $\Delta\alpha > 0$, and in these cases the bonds are less strained than the geometrical angles α_e would suggest. In general, $\Delta\alpha$ provides a measure of

the degree of relaxation of the charge density away from the geometrical contraints imposed by the nuclear framework. In cyclopropane, for example, $\Delta\alpha = 18.8°$, and the deviation of the angle formed by the bond paths from the normal tetrahedral angle is correspondingly less. This difference decreases to 6.1° in cyclobutane and becomes small and negative for five- and six-membered rings. The negative value of $\Delta\alpha$ for cyclohexane brings the bond path angle to within $^1/_2°$ of the tetrahedral angle. The strain energy of cyclopropane is nearly the same as that for cyclobutane in spite of its bond angle being smaller by 30°. This similarity in strain energies can be accounted for, at least in part, by the much greater relaxation of angle strain between the bonds in cyclopropane than between those in cyclobutane. It has also been pointed out[46a] that cyclopropane has no 1-3 nonbonded repulsions, as opposed to the two present in cyclobutane, their presence in the latter molecule being reflected in its longer than normal C-C bond lengths. The absence of 1-3 repulsions in cyclopropane makes inappropriate the use of the C-C-C bending constant of cyclohexane as a basis for postulating a very large strain energy for the former molecule which is then negated by the mechanism of "σ aromaticity".[46b] This argument also ignores the greater C-H bond strength found in cyclopropane as compared to other cycloalkanes, an effect which further compensates for the weaker C-C bonds. A quantitative discussion of the strain energies in these molecules is given in the following paper[23] in terms of the relative energies of the carbon atoms.

The value of $\Delta\alpha$ exceeds 10° only for three-membered rings. The largest values are found for the three-membered rings in tetrahedrane, $\Delta\alpha = 21°$, and for the angle of the three-membered ring formed by the bonds terminating at the central carbon in spiropentane where $\Delta\alpha = 23°$. In spite of these large relaxations, the strain energies for these two molecules are large relative to any comparison with cyclopropane as a prototype. The reason for this being that in tetrahedrane each carbon is common to three three-membered rings, and in spiropentane the central carbon is common to two such rings. These additional constraints result in an increase in the strain energy, and they are present to an even greater extent in bicyclo[1.1.0]butane and in the propellanes. The fusing of three rings to a common bridgehead bond inhibits the relaxation of the bond paths in these latter molecules relative to that found to occur in cyclopropane. This is particularly true for the apex angles of the three-membered rings in [1.1.1]- and [2.1.1]propellane. In the former case, $\Delta\alpha$ is slightly negative and the bond path angle is less than 60°. Both angles in the three-membered ring of [2.2.1]propellane show larger relaxations than in either of the former molecules. The relatively large values of $\Delta\alpha$ for the angles made by the bond paths of the three-membered rings that terminate at a bridgehead carbon in [1.1.1]- and [2.1.1]propellane result in bond path angles that differ by only $\pm1°$ from the tetrahedral angle of 109°. The corresponding bond path angles made by the bond paths from three- and four-membered rings or from two four-membered rings are larger by $\approx8°$ and exhibit smaller relaxations from their geometrical angles. These bridgehead bond path angles can be compared with those in the corresponding bicyclic molecules. The value of 96° for α_b in bicyclo[1.1.1]pentane indicates a greater degree of strain for these bonds than is found in its propellane analogue.

Bond Ellipticity. In a bond with cylindrical symmetry the two negative curvatures of ρ at the bond critical point are of equal magnitude. However, if electronic charge is preferentially accumulated in a given plane along the bond path (as it is for a bond with π-character, for example), then the rate of falloff in ρ from its maximum value ρ_b in the interatomic surface is less along the axis lying in this plane than along the one perpendicular to it, and the magnitude of the corresponding curvature of ρ is smaller. If λ_2 is the value of the smallest curvature, then the quantity $\epsilon = (\lambda_1/\lambda_2 - 1)$, the *ellipticity of the bond*, provides a measure of the extent to which charge is preferentially accumulated in a given plane.[44] The axis of the curvature λ_2, the major axis, determines the relative orientation of this plane within a molecule. For the 6-31G* basis set, the ellipticities of the C-C bonds in ethane, benzene, and ethylene are 0.0, 0.23, and 0.45, respectively, and
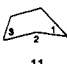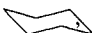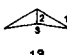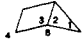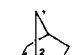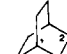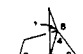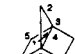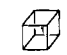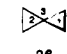
(44) Bader, R. F. W.; Slee, T. S.; Cremer, D.; Kraka, E. *J. Am. Chem. Soc.* **1983**, *105*, 5061.

(45) (a) Wong, J. S.; MacPhall, R. A.; Moore, C. B.; Strauss, H. L. *J. Phys. Chem.* **1982**, *86*, 1478. (b) McKean, D. C.; Biedermann, S.; Burger, H. *Spectrochim. Acta, Part A* **1974**, *30A*, 845.

(46) (a) Wiberg, K. B. *Angew. Chem.* **1986**, *98*, 312. (b) Dewar, M. J. S. *J. Am. Chem. Soc.* **1984**, *106*, 669.

(47) Bader, R. F. W.; Tang, T. H.; Tal, Y.; Biegler-Konig, F. W. *J. Am. Chem. Soc.* **1982**, *104*, 904, 946.

Table II. Geometry and Bond Path Angles[a]

molecule		angle	geometric angle α_e	bond path angle α_b	$\Delta\alpha$ $\alpha_b - \alpha_e$	strain energy, kcal
cyclopropane	**9**	1	60.0	78.84	18.84	27.5
cyclobutane	**10**	1	89.01	95.73	6.72	26.5
cyclopentane	**11**	1	104.55	104.02	−0.53	6.2
		2	105.36	104.43	−0.93	
		3	106.50	105.03	−1.54	
cyclohexane	**12**	1	111.41	110.08	−1.34	0.0
bicyclo[1.1.0]butane	**13**	1	58.99	72.78	13.79	63.9
		2	60.50	76.62	16.12	
		3	97.91	105.07	7.16	
bicyclo[2.1.0]pentane	**14**	1	60.86	79.28	18.42	54.7
		2	59.57	78.30	18.72	
		3	90.84	96.76	5.92	
		4	89.16	95.77	6.61	
		5	110.03	109.72	−0.31	
bicyclo[2.2.0]hexane	**15**	1	90.17	97.01	6.85	51.8
		2	89.91	96.59	6.67	
		3	114.43	112.64	−1.79	
bicyclo[1.1.1]pentane	**16**	1	74.44	84.72	10.27	68.0
		2	87.20	95.85	8.65	
bicyclo[2.1.1]hexane	**17**	1	99.20	100.69	1.48	37.0
		2	101.77	103.46	1.69	
		3	86.11	94.21	8.10	
		4	82.60	90.95	8.35	
bicyclo[2.2.1]heptane	**18**	1	94.37	97.42	3.05	14.4
		2	101.51	102.90	1.39	
		3	108.43	108.69	0.26	
		4	103.13	103.57	0.44	
bicyclo[2.2.2]octane	**19**	1	109.30	108.68	−0.62	7.4
		2	109.64	108.56	−1.08	
[1.1.1]propellane	**20**	1	61.81	59.37	−2.44	98.0
		2	95.98	107.99	12.01	
		3	59.09	69.09	9.99	
[2.1.1]propellane	**21**	1	88.97	93.65	4.69	104.0
		2	91.03	97.91	6.88	
		3	112.30	116.3	4.00	
		4	57.72	67.96	10.25	
		5	97.27	111.45	14.18	
		6	64.57	65.27	0.71	
[2.2.1]propellane	**22**	1	59.18	75.40	16.22	105.0
		2	61.64	74.32	12.68	
		3	112.38	116.43	4.06	
		4	90.86	92.97	2.11	
		5	89.14	96.43	7.30	
		6	128.49	126.57	−1.91	
[2.2.2]propellane	**23**	1	91.15	97.05	5.90	89.0
		2	119.96	118.51	−1.44	
		3	88.85	96.81	7.97	
tetrahedrane	**24**	1	60.00	81.36	21.36	140.0
cubane	**25**	1	90.00	97.43	7.43	154.7
spiropentane	**26**	1	59.24	79.04	19.80	63.2
		2	61.51	84.84	23.33	
		3	137.6	123.02	−14.58	

[a] Angles in degrees.

the major axes of the ellipticities in the latter two cases are perpendicular to the plane of the nuclei as anticipated for molecules with π-bonds.

The chemistry of a three-membered ring is very much a consequence of the high concentration of charge in the interior of the ring relative to that along its bond paths.[44,48] The values of

ρ_r, the value of ρ at a ring critical point, are generally only slightly less than, and in some cases almost equal to, the values of ρ_b for the peripheral bonds in the case of a three-membered ring. In four-membered and larger rings the values of ρ_r are considerably smaller, as the geometrical distance between the bond and ring critical points is greater than in a three-membered ring. (Values of the charge density at ring, ρ_r, and cage, ρ_c, critical points are listed in Table I.) Because electronic charge is concentrated to an appreciable extent over the entire surface of a three-membered ring, the rate of falloff in the charge density from its maximum value along the bond path toward the interior of the ring is much less than its rate of decline in directions perpendicular to the ring surface. Thus the C–C bonds have substantial ellipticities, and their major axes lie in the plane of the ring. In hydrocarbons, this property is unique to a three-membered ring. It accounts for their well-documented ability to act as an unsaturated system with a π-like charge distribution in the plane of the ring that is able to conjugate with a neighboring unsaturated system.[49] This is rationalized within molecular orbital theory through the choice of a particular set of orbitals, the so-called Walsh orbitals.[50] The ellipticity of a C–C bond in cyclopropane is actually greater than that for the double bond in ethylene, indicating that the extent to which charge is preferentially accumulated in the plane of the ring in the former compound is greater than that accumulated in the π-plane of ethylene. Large ellipticities are found for bonds in three-membered rings of the bicyclic and propellane molecules. The very large value, in excess of 7, found for the bridgehead bond in [2.1.1]propellane indicates that it is potentially structurally unstable. The relationship between the value of ϵ and the susceptibility of a bond to rupture is nicely illustrated by the properties of the propellanes.

The structure of a system, as characterized by its molecular graph, is determined by the number of bond, ring, and cage critical points. These are stable critical points in the sense that they retain their properties, and hence the charge density retains its corresponding form as the nuclei are displaced. A structure which contains only stable critical points will thus persist over some range of all possible nuclear motions and is, therefore, a stable structure. When two or more stable critical points coalesce however, the properties of the resulting critical point are unstable with respect to nuclear motions, as is the structure it defines.[28,29,32a] Consider, for example, the coalescence of a bond and a ring critical point such as occurs in the opening of a ring structure. When a bond of a ring structure is extended, the resulting change in ρ causes the critical point of the ring to migrate toward that of the bond. The charge density has a positive curvature at the ring critical point (in the ring surface) and a negative curvature at the bond critical point along their direction of approach. This is illustrated by the densities for the [2.1.1]- and [2.2.1]propellanes in Figure 3. In these two molecules the three-membered-ring critical points are relatively close to the critical point of the bridgehead bond in their equilibrium geometries. The diagram for the [2.2.1] molecule in particular shows in profile the maximum of the bridgehead bond linked to the minimum of the ring critical point of the three-membered ring. The values of ρ at these two critical points are nearly equal (Table I), and they are separated by only 0.46 Å. Consequently, as is evident from the figure, λ_2, the negative curvature of the bond in the direction of the ring critical point, is smaller in magnitude than its perpendicular counterpart λ_1, whose magnitude is essentially unaltered from that of a normal C–C bond. Thus because of the proximity of the three-membered-ring critical point, one of the negative curvatures of the bridgehead bond is decreased in magnitude, and the bond has a large ellipticity.

Upon coalescence of the bond and ring critical points which will occur for some particular extension of the bridgehead bond,

the curvatures of the two critical points, one positive the other negative, must be equal, and hence the curvature of the new critical point formed by their merger must be zero. This new critical point with one zero curvature is unstable—it exists only for this particular value of the bond extension, and at this extension the bond is broken. Since the magnitude of the negative curvature λ_2 decreases during the approach of the critical points and ultimately equals zero on their coalescence, the ellipticity of the bond undergoes a dramatic increase, becoming infinite when the bond is broken.[44,48] Gatti et al.[51] have discussed the relative stability of the substituted [10]annulene vs. the dinorcaradiene structures as a function of the ellipticity of the C_1–C_6 bond which links the bridgehead nuclei in the latter structures.

If the unstable critical point is formed in an isolated ring system, a further extension of the bond causes it to vanish and the ring structure is changed into an open structure, corresponding to the loss of a bond and a ring critical point. The rupture of the bridgehead bond in [1.1.1]propellane transforms the structure into a cage structure similar to that of the related bicyclic compound.[29]

The bridgehead bond in [2.1.1]propellane, with an ellipticity of 7.1, is potentially the most susceptible to rupture. As is clear from Figure 3 and the data in Table I, the values of ρ at the bond critical point and at the two three-membered-ring critical points are of almost equal value, and they are separated by only 0.066 Å. The magnitude of the bond curvature λ_2 is close to zero, the value which signals the formation of an unstable structure through the breaking of the bridgehead bond. Both the bridgehead and a bond of the three-membered ring in [2.1.1]propellane have relatively high ellipticities. Because of symmetry, the bridgehead bond in [1.1.1]propellane does not exhibit any ellipticity. As is evident from Figure 3 and from the data in Table I, however, the ring critical points are only 0.25 Å from the bond critical point, and their values differ by only 0.004 au. As previously demonstrated,[29,47] an extension of the bridgehead bond in this molecule results in the coalescence of the bond and three ring critical points and the formation of an unstable critical point with two zero curvatures. Depending upon the symmetry of the nuclear displacement away from the geometry of the unstable structure, a number of stable structures, including a cage, can be formed.[29] The bonds of the [2.2.2]propellane molecule, since it has only four-membered rings in its structure, do not exhibit significant ellipticities.

While [2.1.1]- and [2.2.1]propellanes are relatively unstable, as suggested by the properties of their charge distributions, and readily undergo polymerization at 50 K, [1.1.1] is the most stable of these propellanes and is considerably more stable than [2.2.2] with respect to thermolysis.[52] Stability is not a function of just the static properties of the equilibrium charge distribution but also depends upon how the distribution changes with the possible nuclear motions. The final comparison of the relative stabilities of the propellane structures is postponed until this dynamic aspect of their properties is presented through a study of the charge relaxations accompanying their nuclear motions.

Laplacian of the Charge Density. Central to the models of molecular geometry and chemical reactivity is the concept of localized pairs of electrons, bonded and nonbonded.[53] In general, aside from core regions, electrons are not spatially localized.[54] Neither the properties of the pair density nor the topology of the total charge distribution offers evidence of localized pairs of electrons, bonded or nonbonded. One may arbitrarily select a set of orbitals which individually show some degree of spatial localization.[55-57] However, only the total density has physical

(48) Cremer, D.; Kraka, E.; Slee, T. S.; Bader, R. F. W.; Lau, C. D. H.; Nguyen-Dang, T. T.; MacDougall, P. J. *J. Am. Chem. Soc.* **1983**, *105*, 5069.

(49) Capon, B.; McManus, S. P. *Neighboring Group Participation*; Plenum: New York, 1976.

(50) Walsh, A. D. *Nature (London)* **1947**, *159*, 712. Walsh, A. D. *Trans. Faraday Soc.* **1949**, *45*, 179.
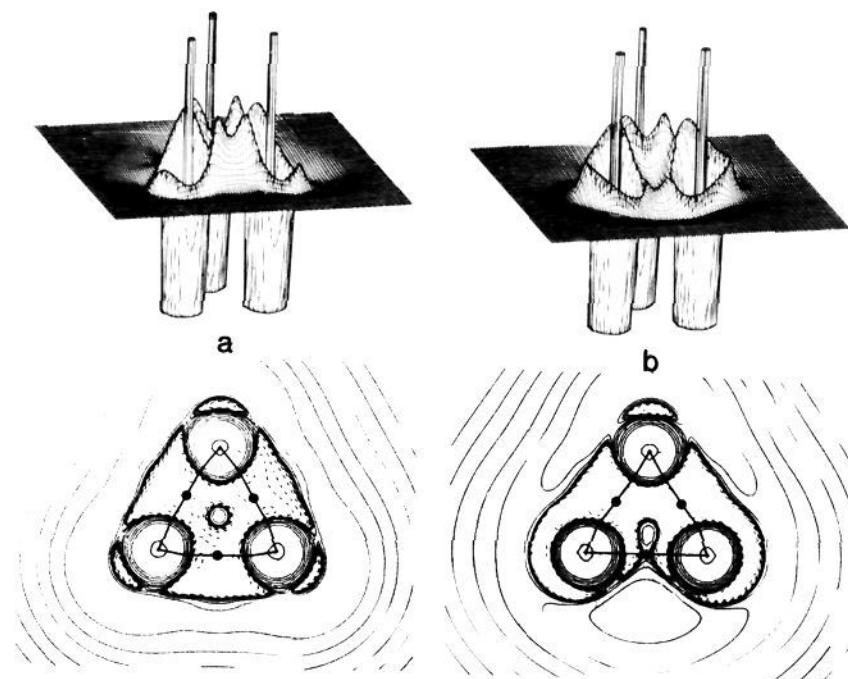
(51) Gatti, C.; Barzaghi, M.; Simonetta, M. *J. Am. Chem. Soc.* **1985**, *107*, 878.

(52) Eaton, P. E.; Temme, G. H., Jr. *J. Am. Chem. Soc.* **1973**, *95*, 7508. Eaton and Temme found E_a = 22 kcal/mol for the thermolysis of [2.2.2]-propellane, whereas for [1.1.1]propellane it is 30 kcal/mol.[7]

(53) Lewis, G. N. *J. Am. Chem. Soc.* **1916**, *38*, 762.

(54) Bader, R. F. W.; Stephens, M. E. *J. Am. Chem. Soc.* **1975**, *97*, 7391.

(55) Lennard-Jones, J. E. *J. Chem. Phys.* **1952**, *20*, 1024. Lennard-Jones, J. E. *Proc. R. Soc. London, A* **1949**, *A198*, 1, 14.

(56) Edmiston, C.; Ruedenberg, K. *Rev. Mod. Phys.* **1963**, *35*, 457. Edmiston, C.; Ruedenberg, K. *Fortschr. Chem. Forsch.* **1971**, *23*, 31.

Figure 4. Contour maps of the Laplacian of the charge density overlaid with bond paths, and corresponding relief maps of the negative of this function: (a) plane of the carbon nuclei in cyclopropane, (b) plane of a three-membered ring in [1.1.1]propellane. Dashed contours denote negative values. The spike-like charge concentration at each carbon nucleus has been terminated at -2.0 au. The values of $\nabla^2\rho$ at the bond critical points are given in Table I, and at a bonded maximum to another carbon in a the value is ~0.89 au. In b the value at a bridgehead bonded maximum is -0.13 au, -0.89 au at the bonded maximum with a bridging carbon, and -0.40 au at the nonbonded charge concentration.

meaning, and every set of orbital densities for a system, no matter how the orbitals are chosen, sum to the same total density. What is indeed remarkable is that when one sums the individual orbital densities, their nodes and all suggestions of spatially localized patterns of charge dissolve to yield the relatively simple topology exhibited by the total charge density. This topology, as discussed above, provides a faithful mapping of the chemical concepts of atoms, bonds, and structure, but it must be recognized that it does not provide any indication of maxima that would correspond to the electron pairs of the Lewis model. The physical basis of this most important of all chemical models is one level of abstraction above the visible topology of ρ and appears instead in the topology of the Laplacian of ρ.[58]

The Laplacian of ρ is the sum of its three principal curvatures at each point in space, the quantity $\nabla^2\rho(r)$. When $\nabla^2\rho(r) < 0$, the value of the charge density at the point r is greater than the value of $\rho(r)$ averaged over all neighboring points in space, and when $\nabla^2\rho(r) > 0$, $\rho(r)$ is less than this averaged value. Thus a maximum (a minimum) in $-\nabla^2\rho(r)$ means that electronic charge is locally concentrated (locally depleted) in that region of space even though the charge density itself exhibits no corresponding maximum (minimum).[59] One may think of $\nabla^2\rho$ as providing a measure of the extent to which the charge density is locally compressed or expanded. This property of ρ must be distinguished from local maxima and minima in ρ itself.

The Laplacian of ρ recovers the shell structure of an atom by displaying a corresponding number of shells of charge concentration and charge depletion. On bonding, the uniform valence shell of charge concentration of a free atom is distorted so as to form "lumps" and "holes" in this shell.[58] The maxima in $-\nabla^2\rho$ recover the lumps anticipated in terms of the Lewis electron pair model or as surmised to exist in Gillespie's VSEPR model of molecular geometry.[60] These *local concentrations of charge*

(57) Boys, S. F. *Rev. Mod. Phys.* **1960**, *32*, 296. Foster, J. M.; Boys, S. F. *Rev. Mod. Phys.* **1960**, *32*, 300.
(58) Bader, R. F. W.; MacDougall, P. J.; Lau, C. D. H. *J. Am. Chem. Soc.* **1984**, *106*, 1594.
(59) The critical points in the Laplacian of ρ are determined by a program which finds the points where $\nabla(\nabla^2\rho) = 0$. These points are classified as maxima, minima, or saddles by determining the curvatures of $\nabla^2\rho$ at the critical point, the roots of $\nabla^2(\nabla^2\rho)$.
(60) Gillespie, R. J. *Molecular Geometry*; Van Nostrand–Reinhold: London, 1972.

determine the sites of electrophilic attack. They also correlate with the regions where the HOMO is most concentrated. The points where $-\nabla^2\rho$ attains its minimum values locate the holes in the valence shell charge concentration. These holes, since they give direct access to the core of the atom, are the sites of nucleophilic attack. They correlate with the regions of space where the LUMO is most concentrated.[61,62] These properties of the Laplacian are illustrated in Figure 4 for cyclopropane and [1.1.1]propellane.

The Laplacian of ρ plays a dominant role in the theory of atoms in molecules.[25] The quantum condition of zero flux in the gradient vector of ρ that defines the atom, when integrated over the surface of an atom Ω, yields a constraint on the atomic average of the Laplacian of ρ (eq 1). According to eq 1 if charge is concentrated

$$\oint dS\nabla\rho\cdot\mathbf{n} = \int_\Omega \nabla^2\rho d\tau = 0 \tag{1}$$

in some regions of an atom, it must be depleted to a corresponding extent in others, since the integral of the Laplacian over an atom must vanish. This property is common to all atoms, free or bound. The Laplacian appears in the local expression for the virial theorem:[25,63]

$$(\hbar^2/4m)\nabla^2\rho(r) = V(r) + 2G(r) \tag{2}$$

The quantity $V(r)$ when integrated over an atom or over all space yields the corresponding value of the potential energy and is, therefore, the potential energy density. Correspondingly, $G(r)$ is the kinetic energy density, since its integration over an atom or over all space yields the kinetic energy T. Since the integral of the Laplacian of ρ over an atom Ω or over the total system vanishes, integration of eq 2 yields the virial theorem for an atom, $V(\Omega) + 2T(\Omega) = 0$, or for the total system, $V + 2T = 0$. Since $G(r) > 0$ and $V(r) < 0$, eq 2 demonstrates that the lowering of the potential energy dominates the energy in those regions of space where electronic charge is concentrated or compressed, i.e., where $\nabla^2\rho < 0$.[36]

The charge density is a maximum in an interatomic surface at the bond critical point. The two curvatures of ρ perpendicular to the bond path at the bond critical point, λ_1 and λ_2 in Table I, are therefore negative, and charge is locally concentrated in the surface at this point. The charge density is a minimum at the same point along the bond path, the third curvature of ρ at the bond critical point λ_3 being positive. Charge is locally depleted at the critical point with respect to neighboring points on the bond path. Thus the formation of an interatomic surface and a chemical bond is the result of a competition between the perpendicular contractions of ρ which lead to a contraction or compression of charge along the bond path and the parallel expansion of ρ which leads to its depletion in the surface and to its separate concentration in the basins of the neighboring nuclei.[36] The sign of $\nabla^2\rho$ at the bond critical point determines which of the two competing effects is dominant.

When $\nabla^2\rho < 0$ and is large in magnitude, a perpendicular contractions of ρ dominate the interaction and electronic charge is concentrated between the nuclei along the bond path. The result is a sharing of electronic charge between the atoms as is found in covalent or polar bonds. This is the situation for all of the C–H and all of the C–C bonds of the hydrocarbons with the exception of the bridgehead bonds in [2.1.1]- and [1.1.1]propellane. Figure 5a for ethane or Figure 4a for cyclopropane illustrates the manner in which the valence electronic charge is concentrated between the nuclei in shared interactions, a sharing which bridges the basins of the neighboring atoms. According to eq 2, these bonds achieve their stability through the lowering of the potential energy of the electronic charge that is concentrated between the nuclei and shared by both atoms.[36]

(61) Bader, R. F. W.; MacDougall, P. J. *J. Am. Chem. Soc.* **1985**, *107*, 6788.
(62) Tang, T. H.; Bader, R. F. W.; MacDougall, P. J. *Inorg. Chem.* **1985**, *24*, 2047.
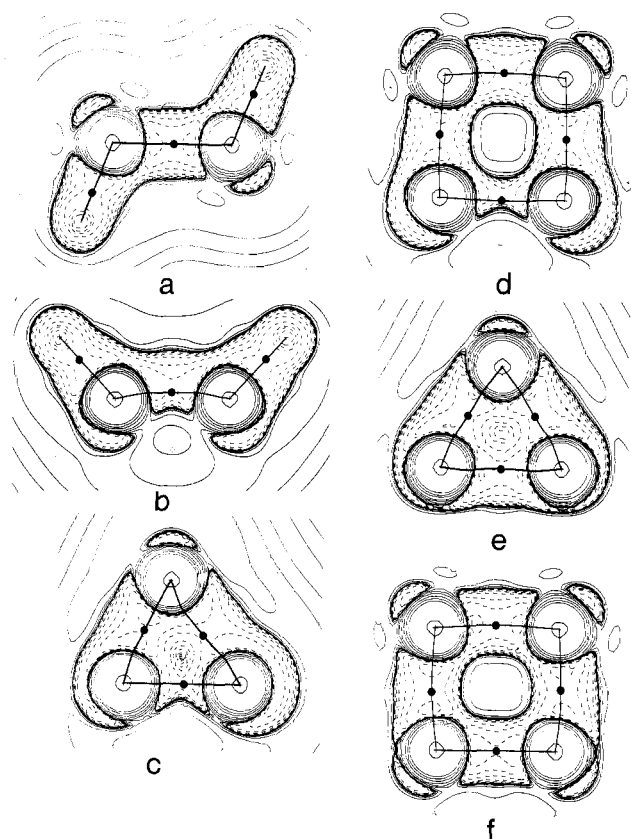(63) Bader, R. F. W. *J. Chem. Phys.* **1980**, *73*, 2871.

Figure 5. Contour maps of the Laplacian of the charge density overlaid with bond paths: (a) H–C–C–H plane of ethane, (b) H–C–C–H symmetry plane containing bridgehead bond in bicyclo[1.1.0]butane, (c) distorted geometry of [1.1.1]propellane in which the bridgehead nuclei are displaced in an opposite direction from the bridging methylene groups, (d) plane of four-membered ring in [2.1.1]propellane, (e) plane of three-membered ring in [2.2.1]propellane, (f) plane of four-membered ring in [2.2.2]propellane. See Table I for values of $\nabla^2\rho$ at the bond critical points. The value at a nonbonded charge concentration on a bridgehead carbon in d is –0.51 au and in b is –0.37 au. The value of a bonded charge concentration on a C–C bond axis is –1.03 au in a, –0.72 au in b, –0.29 au for a bridgehead bond, and –1.05 au for the second bond from the bridgehead in d. Corresponding pairs of values for e are –0.86 and –0.84 au and for f are –1.29 and –0.99 au.

The value of $\nabla^2\rho_b$ for the C–H bonds parallels ρ_b in its behavior, becoming more negative as the value of ρ_b increases. The relatively large value of ρ_b found for H bonded to a geometrically strained carbon, as in cyclopropane, tetrahedrane, or [1.1.1]propellane, is a result of an increase in the degree of contraction of the charge density in the interatomic surface toward the bond path.

The values of $\nabla^2\rho$ and its individual components show only minor variations for the majority of the C–C bonds. The magnitude of $\nabla^2\rho$ for bonds with significant ellipticities as found in cyclopropane and in three-membered rings of bicyclic structures is reduced as a result of the softening of one of the negative curvatures. As discussed above, electronic charge is delocalized over the ring surface as a consequence of this softening. A comparison of the contour maps of $\nabla^2\rho$ for a four-membered ring and those for cyclopropane, Figures 4 and 5, shows that in the latter, all three nuclei are bound by what is essentially a common charge concentration in the ring interior as opposed to the former case where the dominant concentrations are separately localized along the bonds. Thus the significant ellipticities of the perimeter bonds in cyclopropane lead to a delocalization of charge over the surface of the ring. The extent of this delocalization and the accompanying concentration of charge in the ring interior is reflected in the outward curvature of the C–C bond paths and in their unusually short bond lengths. The concentration of charge exerts attractive forces on all three ring nuclei and simultaneously lowers their potential energy. Therefore, while the small bond angles of a three-membered ring result in strain, the amount of

strain energy is less than anticipated on this basis alone because of the presence of the π-like delocalized charge and its sharing by all of the ring nuclei unique to a three-membered ring.[36,64]

It has been shown that the enhanced electrophilic reactivity of cyclopropanes over cyclopentanes and similar hydrocarbons is not related to the release of strain energy which accompanies the rupture of a C–C bond on acetolysis.[65] Cyclopropane and cyclobutane have similar strain energies and enthalpies of acetolysis, yet the latter is essentially inert while the former has a moderate reactivity. The susceptibility of cyclopropanes to protonation has the same origin as that for an olefin—bonds with large ellipticities and resulting concentrations of less tightly bound electronic charge, π-density in an olefin and in-plane delocalized charge for the three-membered rings.

When $\nabla^2\rho > 0$, one has the other limiting type of atomic interaction—an interaction dominated by contractions of the charge density toward each of the nuclei as reflected in the dominance of the positive curvature of ρ, λ_3 along the bond path. They are called closed-shell interactions as they typify interactions between closed-shell atoms as found in noble gas repulsive states, ionic bonds, hydrogen bonds, van der Waals molecules and the relatively long bonds found between what are formally closed-shell atoms[62] in compounds such as S_4N_4 and S_8^{2+}. The dominance of the positive curvature of ρ along the atomic interaction line is a consequence of the Pauli exclusion principle, which leads to a separate concentration of charge in each atomic basin.[36] The electronic energy of these systems is lowered by the charge concentrated in the basin of each atom. One also observes a progressive change from an interaction dominated by the perpendicular contractions to one dominated by the parallel contraction of ρ for the bond between identical but progressively more electronegative atoms. Thus $\nabla^2\rho$ is negative for the C–C bond in ethane and for the N–N bond in H_2NNH_2, less negative for the O–O bond in HOOH, and positive for F–F. The positive, parallel curvature λ_3 increases dramatically in this isoelectronic series from 0.29 in ethane to 1.88 au in F_2. The charge density of a bound fluorine atom is both tightly bound and strongly localized within its boundaries. This is a favorable trait for an ionic interaction but the antithesis of that required for a shared homopolar interaction, and the F_2 bond is relatively weak.[36] The charge density of each fluorine atom in F_2 is polarized toward the other nucleus, and the molecule is bound by the net accumulation of charge in the binding region of each atom.

The trend in $\nabla^2\rho_b$ toward positive values for bonds between atoms of increasing electronegativity parallels the observed decrease in the amount of charge accumulated in the binding regions of such bonds as determined by a map of the deformation density, $\Delta\rho$.[22] Thus $\Delta\rho > 0$ in the binding region of a normal C–C bond where the interaction is dominated by a shared accumulation of charge between the nuclei. Its value becomes smaller and eventually negative as the bonded atoms become more electronegative, and the interaction is increasingly dominated by the separate localization of charge in each of the atomic basins, as, for example, in bonds between oxygen atoms. Dunitz and Seiler[22] also ascribe this trend in the behavior of $\Delta\rho$ in the binding region to the increasing importance of the exclusion principle and its effect of separately localizing charge on each of the atoms. It is found that an experimental density difference map does not show a buildup of charge between the bridgehead nuclei in a [3.1.1]propellane,[21] and in agreement with the above observation, the value of $\nabla^2\rho$ is also positive or close to zero for the bridgehead bond in a propellane with at least two three-membered rings (Table I).

The bridgehead bonds in the propellanes exhibit the greatest variation in properties of the bonds encountered in this study, Figures 4 and 5. The value of $\nabla^2\rho$ at the bridgehead bond critical point is negative and large in magnitude for [2.2.2]propellane, as anticipated for a bond of order greater than unity. This bond

(64) Bader, R. F. W. *Chemical Applications of Topological Graph Theory*; King, R. B., Ed.; Elsevier: New York, 1983. Cremer, D.; Kraka, E. *J. Am. Chem. Soc.* **1985**, *107*, 3800.

(65) Wiberg, K. B.; Kass, S. R. *J. Am. Chem. Soc.* **1985**, *107*, 988.

differs from a normal bond with $n > 1$ in that it possesses the largest value for the positive curvature of ρ, λ_3. Usually this measure of the curvature of ρ along the bond path decreases (the curvature is softened) as more charge is accumulated between the nuclei. Thus there is a relatively large tension in the charge density along the bridgehead bond path tending to separately concentrate the density in the two atomic basins. The value of $\nabla^2\rho$ for the bridgehead bond becomes increasingly less negative through the series as the number of three-membered rings increases. Its value is close to zero in [2.1.1]propellane and slightly positive in [1.1.1]propellane. The bridgehead bonds in these two molecules are intermediate between a shared interaction and one dominated by the separate localization of charge in each of the atomic basins. The resulting pattern of charge concentration and removal is different from that for a normal C–C bond, and the chemistry of the bridgehead carbon atoms is correspondingly altered.

The valence shell of charge concentration exhibits local maxima equal in number to the number of bonded and nonbonded Lewis pairs, and their relative orientation and sizes are as anticipated on the basis of the VSEPR model of molecular geometry.[60] Carbon in methane has four tetrahedrally directed maxima, nitrogen in ammonia has three bonded maxima and one larger, broader nonbonded maxima, and oxygen in water has two bonded and two nonbonded maxima. This parallelism between the model of bonded and nonbonded pairs and the local maxima in the valence shell of charge concentration as defined by the Laplacian of the charge density is always found.[58] Thus the chlorine atom in ClF_3 has three bonded maxima, two axial and one equatorial, and two larger, broader equatorially placed nonbonded maxima, as anticipated on the basis of its T-shaped geometry.[60]

In addition to the maxima, local minima exist on the surface of the sphere of charge concentration in the valence shell of a bound atom. The maxima are linked by lines originating at intervening saddle points in $\nabla^2\rho$, similar to the bond paths as determined by the topology of ρ itself. In the case of a carbon atom in methane or ethane, the result is a tetrahedron with curved faces. In the center of each face and opposite to a bonded maximum there is a local minimum in $\nabla^2\rho$. This arrangement of maxima linked by lines which encompass local minima is called an atomic graph.[61] The relief and contour maps for the plane of the carbon nuclei in cyclopropane (Figure 4a) show two of the four bonded maximum on each carbon where $\nabla^2\rho$ is very negative, one for each C–C bond, and opposite each is a minimum where $\nabla^2\rho$ is positive. Although slightly distorted from a regular tetrahedron, this pattern is similar to that for a carbon in ethane, Figure 5a.

In [2.2.2]propellane the four bonded maxima of a bridgehead carbon atom lie approximately on the corresponding internuclear axes. While the atomic graph of this atom is distorted from the regular tetrahedral arrangement, the basic pattern survives. The most noticeable difference is that $\nabla^2\rho$ is very slightly negative, rather than positive, at the center of the face opposite the bridgehead bond.

Because the arrangement of the four bonded maxima on the bridgehead carbon in [1.1.1]propellane reflects its inverted geometry, the structure and nature of the atomic graph for this atom are greatly altered from the regular pattern, as can be seen by comparing its Laplacian plot, Figure 4b with that for cyclopropane, Figure 4a. The shift of all four bonded maxima to one side of a plane causes the three saddle points whose lines define the face opposite the bridgehead bond to coalesce with the local minimum at the face center to produce a broad local maximum in $-\nabla^2\rho$, a nonbonded concentration of charge. The magnitude of the Laplacian is greater at this point in [1.1.1]propellane than it is for the bonded maximum directed at the opposing bridgehead carbon.[66] Thus the valence shell of a bridgehead carbon atom

in [1.1.1]propellane exhibits five local charge concentrations, four bonded and one nonbonded. The exposed bridgehead nonbonded charge concentration is a site of electrophilic attack. Its ease of protonation explains the pronounced susceptibility of [1.1.1]-propellane to acetolysis.[7b] A display of the Laplacian of ρ for [1.1.1]propellane that has been displaced in the manner of an antisymmetric stretch of the carbon skeletal framework is shown in Figure 5c. This is a very intense low-frequency motion[7b] and, as discussed below, is the most facile of the framework motions for this molecule. Its effect is to shorten the bridgehead bond by concentrating more charge between these nuclei and to greatly enhance the nonbonded concentration of charge on a bridgehead carbon. Thus this dynamic property of the charge density further enhances the reactivity of [1.1.1]propellane toward electrophiles.

The bridgehead carbons in [2.1.1]propellane and bicyclo-[1.1.0]butane also exhibit inverted geometries, and they possess a relatively large charge concentration, as opposed to the normal depletion, in the center of the face opposite the bridgehead bond, Figure 5b,d. The principal concentration of charge in the non-bonded regions of these carbons does not lie on the bridgehead axis as it does in [1.1.1]propellane. While not as accessible, these charge concentrations serve as centers of electrophilic attack, and [2.1.1]propellane should be, and bicyclo[1.1.0]butane is, susceptible to acetolysis.[67] This concentration is gone in [2.2.1]-propellane, which approaches the more regular pattern found in [2.2.2]propellane.

According to eq 2, the charge concentrations for which the Laplacian of ρ is least negative will be the least tightly bound, and one observes that such concentrations correlate spatially with the regions where the HOMO is most concentrated.[61] For [1.1.1]propellane the least tightly bound charge concentrations lie on the axis of the bridgehead bond, and their polarization into the nonbonded regions of the bridgehead atoms mimics the properties of the HOMO. Newton and Schulman[9] noted that when the orbitals for this molecule were transformed into an equivalent set, a negative overlap population was obtained for the orbital localized between the bridgehead nuclei. As already noted, Jackson and Allen[10] emphasize the extent to which the HOMO accumulates charge in nonbonded regions. Honegger et al.[68] have determined that the molecular ion formed in the lowest energy photoejection of an electron from [1.1.1]propellane, which according to the orbital model comes from the HOMO, has an equilibrium geometry which differs only minutely from that of the parent molecule. They argue that this lack of a structural change can be viewed as a consequence of the nonbonding nature of the HOMO. In terms of the properties of the total charge distribution, a line of maximum charge density links the bridgehead nuclei in the equilibrium geometry where the forces on the nuclei vanish and the bridgehead nuclei are bonded. As already discussed, however, the nature of this bonding differs from that of a normal C–C bond. Within the framework of the orbital model these differences are primarily a consequence of the density of the HOMO,[9,10] and in terms of the properties of the total charge density, they are made most evident in the Laplacian distribution.

The presence of the nonbonded charge concentrations on the bridgehead carbons of [1.1.1]propellane (Figure 4b) does not imply that the net forces exerted on these nuclei by the bridgehead density are antibinding rather than binding. The atomic dipole $\mu(\Omega)^{69}$ of a bridgehead carbon in [1.1.1]propellane is large and is directed away from the second nucleus, being dominated by the diffuse concentration of nonbonded charge. The force exerted on the bridgehead nucleus by its own charge density, the atomic force[69] $F(\Omega)$, is, however, binding, being dominated by density closer to the nucleus. This force is directed at the other bridgehead nucleus to which it is linked by a bond path. This pattern of atomic moments—dipolar directed away from the electric field directed

(66) The reader is cautioned against interpreting the small charge concentration in the nonbonded region of a carbon in cyclopropane as a local maximum similar to the one shown for [1.1.1]propellane, Figure 4. The third curvature of $-\nabla^2\rho$ at this point in cyclopropane is positive and it is a saddle in $\nabla^2\rho$ linking the two maxima for the C–H bonds, the same as that shown for the carbon in ethane, Figure 5a.

(67) Wiberg, K. B.; Szeimies, G. *J. Am. Chem. Soc.* **1970**, *92*, 571.

(68) Honegger, E.; Huber, H.; Heilbronner, E.; Dailey, W. P.; Wiberg, K. B. *J. Am. Chem. Soc.* **1985**, *107*, 7172.

(69) The atomic dipole $\mu(\Omega)$ is the average of the position vector r from the nucleus over the density in the basin of atom Ω. The atomic force $F(\Omega)$ is the average of the vector $Z_\Omega r/r^3$ over the density in the basin of atom Ω.

Table III. Atomic Dipoles and Forces

molecule and atom Ω^a	$\bar{\mu}(\Omega)$, au	$\vec{F}(\Omega)$, au
C in C_2	−0.172	+0.931
N in N_2	−0.590	+1.671
F in F_2	−0.197	+0.520
N in N_2	−0.623	+1.123
C_b in [1.1.1]propellane	−0.970	+0.435
C_b in [2.2.2]propellane	−0.279	+0.447

^{a} The first three sets of results are calculated from functions close to the Hartree–Fock limit (Cade, P. E.; Wahl, A. C. *At. Data Nucl. Data Tables* **1974**, *13*, 339). The remaining are from 6-31G*/6-31G* functions which, while quantitatively less accurate than the near Hartree–Fock functions in their description of atomic moments, yield qualitatively similar results. A negative sign for $\bar{\mu}$ or $\vec{F}$ denotes a vector directed away from its bonded partner.

toward the bonded nucleus—is not unique to the bridgehead carbons but is the normal pattern for the atoms in C_2, N_2, O_2, and F_2, as evidenced by the data presented in Table III. The largest atomic moments in this set are for the nitrogen atom, which possesses an axial "lone pair" in N_2 and the strongest bond. Thus the bridgehead carbons in [1.1.1]propellane differ not in kind but only in the degree of the polarizations, the dipole being larger and the binding force smaller in magnitude than those found for atoms in more strongly bound systems. In [2.2.2]propellane the dipolar moment is greatly reduced in magnitude. The binding force is slightly larger, and the bridgehead carbons do not exhibit the special properties they do in [1.1.1]propellane.

V. Changes in the Charge Density

The reactivity and stability of a structure are determined not only by the properties of its equilibrium charge distribution but by how the distribution changes as the nuclei are displaced. Second-order perturbation theory can be used to predict the essential features of the change or relaxation in the electronic charge density for a given displacement of the nuclei.[70,71] This is done by approximating the relaxation in ρ by the transition density obtained by a mixing in of the lowest energy excited state of appropriate symmetry, the symmetry being determined by the perturbing nuclear displacement. Assuming that the largest relaxation in ρ is caused by mixing in the excited state of lowest energy, one is able to determine the nuclear displacement that results in the smallest energy increase. By predicting the stretching mode with the lowest force constant, the method may be used to predict the dissociative pathways of unimolecular reactions[69] and the symmetries of equilibrium geometries.[72,73] When used in conjunction with the properties of the Laplacian of the charge density in determining the initial approach of the reactants, the method provides a basis for predicting chemical reaction pathways.[61]

The most strained of the propellanes and other related compounds such as bicyclo[1.1.0]butane exhibit a characteristic and intense low-frequency absorption band in the infrared spectrum.[7b,74,75] This band has been shown to correspond to an antisymmetric C–C stretching motion in which the bridgehead nuclei move in opposition to the remainder of the carbon framework. The presence of this motion is accounted for by the above perturbation theory, and a knowledge of how the charge density changes during motion of the bridgehead nuclei gives further insight into the reactivities of the propellanes and their relative thermal stabilities.

The transition density ρ_{ok} obtained by mixing the excited-state function ϕ_k with the ground-state function ϕ_o is defined as is the normal charge density, except that the product $\{\phi_o\}^2$ is replaced

(70) Bader, R. F. W. *Mol. Phys.* **1960**, *3*, 137.
(71) Bader, R. F. W. *Can. J. Chem.* **1962**, *40*, 1164.
(72) Pearson, R. G. *Symmetry Rules for Chemical Reactions*; Wiley: New York, 1976.
(73) Bartell, L. S. *J. Chem. Educ.* **1968**, *45*, 754.
(74) Wiberg, K. B.; Peters, K. S. *Spectrochim. Acta, Part A* **1977**, *33A*, 261. Wiberg, K. B.; Sturmer, D. *Spectrochim. Acta, Part A* **1975**, *31A*, 57.
(75) Wiberg, K. B.; Walker, F. H.; Pratt, W. E.; Michl, J. *J. Am. Chem. Soc.* **1983**, *105*, 3638.
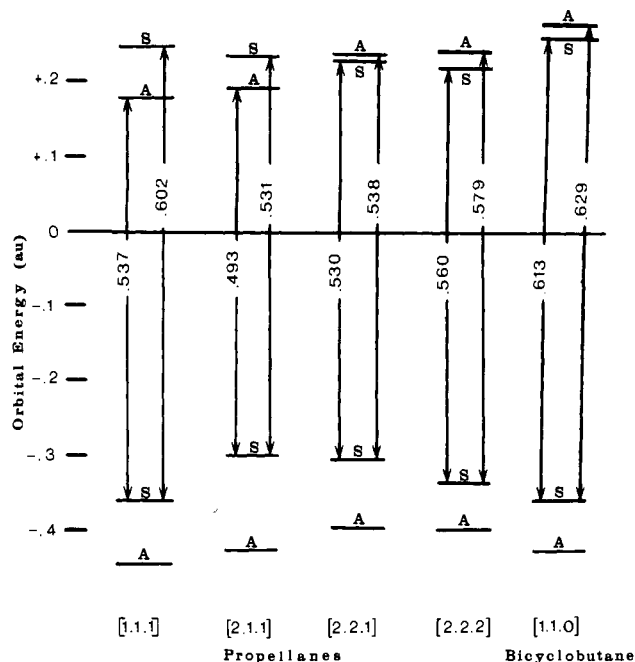

Figure 6. Orbital energy level diagram for propellanes and bicyclobutane. The labels S and A denote symmetric and antisymmetric behavior, respectively, with respect to the symmetry plane bisecting the bridgehead bond.

by the product $\{\phi_o\phi_k\}$ for real functions. Because of the orthogonality of state functions, ρ_{ok} does not integrate to an absolute amount of charge but rather it describes a change in the charge distribution, charge being removed from regions where $\rho_{ok} < 0$ and being placed in regions where $\rho_{ok} > 0$. If ϕ_o is expressed as a single determinant and if ϕ_k is expressed in terms of the occupied and virtual orbitals obtained in the calculation of ϕ_o, then ρ_{ok} reduces to a simple product of orbitals, those that are singly occupied in ϕ_k. If ϕ_o is totally symmetric as it is in the cases of interest here, then ρ_{ok} has the same symmetry as does the excited state ϕ_k, and it will approximate the relaxation for a nuclear mode Q_i of identical symmetry. The charge density, correct to first order, expressed as a function of Q_i, the displacement from equilibrium along coordinate i, is

$$\rho(Q_i) = \rho_{oo} + C(Q_i)\rho_{ok}$$

where ρ_{oo} is the equilibrium charge density determined by ϕ_o, and the coefficient which determines the extent of the relaxation is given by

$$C(Q_i) = 2\{V_{ok}{}^i/(E_k - E_o)\}Q_i$$

The quantity $V_{ok}{}^i$ measures the forces exerted on the nuclei by the transition density. Because of the appearance in the denominator of the difference in energies of the two states, one anticipates that the largest relaxation in the charge density will be obtained for the mode Q_i which is of the appropriate symmetry to mix in the lowest lying of the excited states. The transition density ρ_{ok} determines the transition dipole, the change in the electric dipole moment caused by the displacement Q_i, and the intensity of the mode is proportional to the square of the transition dipole.

Figure 6 summarizes the symmetry properties of the highest energy occupied and lowest energy virtual orbitals of the propellanes. They are labeled as symmetric (S) or antisymmetric (A) with respect to the symmetry plane that bisects the bridgehead bond. In each case the HOMO is S, being primarily the in-phase overlap of $p\sigma$ orbitals on the bridgehead carbons. The order of the symmetries of the LUMO and LUMO+1, however, switch from A and S, respectively, for [1.1.1]propellane to S and A for [2.2.2]propellane. The antisymmetric lowest energy virtual orbital is in every case the antibonding counterpart of the HOMO. The symmetric one has very large s contributions on each carbon and is antibonding between every carbon and its associated hydrogens.

PROPELLANE

[1.1.1]   [2.2.2]

[1.1.0] BICYCLOBUTANE

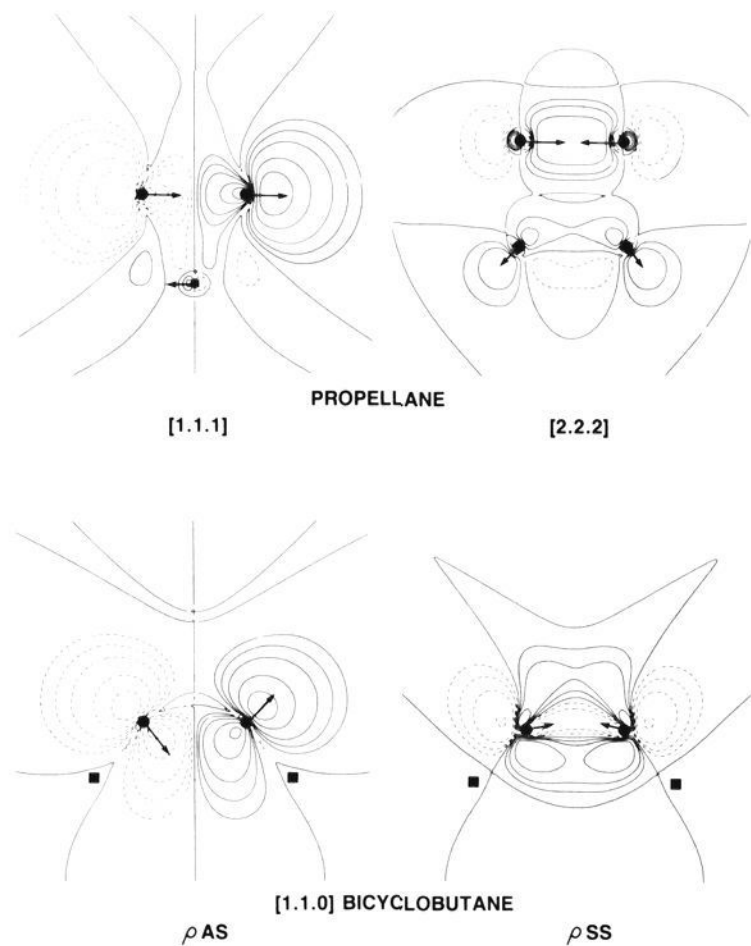ρ AS ρ SS

Figure 7. Contour maps of transition densities for bridgehead bonds and arrows indicating the nuclear motions they induce. Solid contours denote an increase, dashed contours a decrease, in the electronic charge density. Carbon nuclei are denoted by dots, hydrogen nuclei by squares. See Figure 8 for relief maps of the propellane densities.

The energy difference $E_k - E_o$ is approximated by the difference in the energies of the orbitals appearing in the transition density and is referred to as $\Delta\epsilon$. The energy gap between the HOMO and its adjacent occupied orbital is in every case greater than the gap between the two virtual orbitals. The antisymmetric transition density ρ_{AS} is lowest in energy for [1.1.1]- and [2.1.1]propellane. The A and S virtual orbitals are nearly degenerate in [2.2.1]-propellane, and their order is reversed for this molecule and for [2.2.2]propellane. For these molecules the lowest energy transition density is ρ_{SS}.

The symmetric and antisymmetric transition densities are illustrated in Figures 7 and 8. All the relief maps in Figure 8 are drawn to the same vertical scale, and they provide a relative measure of the intensity of ρ_{ok}. The density ρ_{AS} decreases slightly in intensity while that of ρ_{SS} increases dramatically through the series from [1.1.1]- to [2.2.2]propellane. With the exception of [2.1.1]propellane, both ρ_{AS} and ρ_{SS} are in every case most intense in the region of the bridgehead bond. The antisymmetric charge relaxation corresponds to a large transfer of charge from one bridgehead atom to the other and to the creation of an identically directed dipole on each of these atoms. Smaller and oppositely directed dipoles are created and centered on each of the other carbon nuclei. This flow of charge exerts forces on the nuclei such that the bridgehead and the other framework atoms move along parallel axes but in opposite directions, as illustrated by the A_2'' motion of [1.1.1]propellane in Figure 7. The symmetric relaxation of charge concentrates density in the bridgehead bond or removes it from that region for a reverse motion of the nuclei. The symmetric nuclear motion induced by this density change is illustrated by the A_1' symmetric stretch in [2.2.2]propellane, Figure 7.

The antisymmetric transition density ρ_{AS} is predicted to be the most easily induced change in the charge distribution of [1.1.1]propellane, and the corresponding transition dipole is very large, Figures 7 and 8. Thus this molecule should possess a very strong low lying infrared band of A_2'' symmetry, which is indeed the case.[7b] This vibration is predicted and found to be the most facile of the skeletal stretches. The effect of this mode on the molecule is modeled by a calculation in which the center of the bridgehead bond is displaced 0.02 Å from the σ_h symmetry plane of the equilibrium geometry, the bridgehead separation and the

|1.1.1|

|2.1.1|

|2.2.1|

|2.2.2|

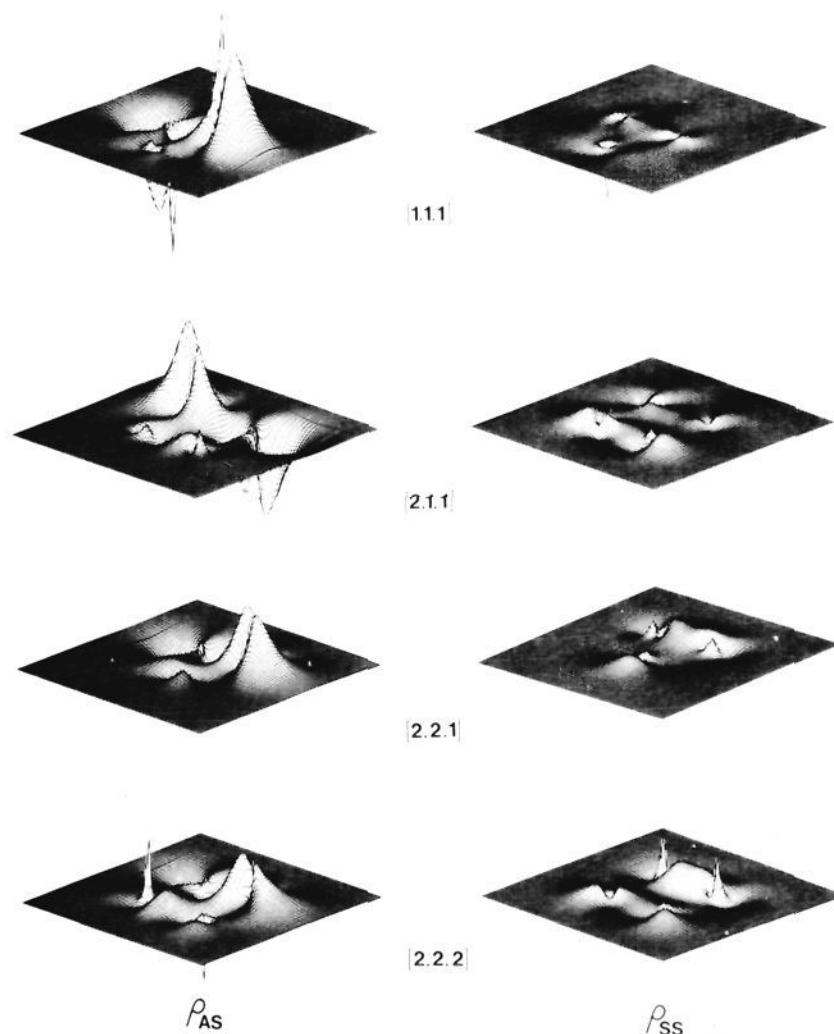ρ_{AS} ρ_{SS}

Figure 8. Relief maps of the lowest energy symmetric and antisymmetric transition densities for the propellanes. A plane of a three-membered ring is shown for [1.1.1]- and [2.2.1]propellane and of a four-membered ring for [2.1.1]- and [2.2.2]propellane. Contour maps of ρ_{AS} for [1.1.1]propellane and of ρ_{SS} for [2.2.2]propellane are shown in Figure 7. The antisymmetric density is most intense for the bridgehead bond in each molecule.

distances of the three apical carbon nuclei from the original center of symmetry being reoptimized. The bridgehead separation was found to decrease by 0.0504 Å and the apical distance to increase by 0.0162 Å. The energy increases by 9.0 kcal/mol. Thus this most facile charge relaxation leads to a strengthening and shortening of the bridgehead bond. The bond order is increased to 0.82, and the Laplacian distribution, Figure 5c, indicates a significant increase in the extent of charge accumulation between the nuclei and an enhancement in a nonbonded charge concentration that alternates between the bridgehead atoms, as anticipated from the form of ρ_{AS}.

The intensity of the symmetric charge relaxation increases through the series, and the symmetric stretch is the most facile of the carbon framework motions for [2.2.2]propellane. The extension of the bridgehead bond as occurs in this motion results in a weakening of this bond as the corresponding transition density (reverse the signs of the contours in Figure 7) transfers charge density from the binding of the antibinding region. Thus while the bridgehead bond of [2.2.2]propellane has the highest bond order in the static equilibrium geometries, it is dynamically more susceptible to thermal rupture than the corresponding bond in [1.1.1]propellane. In [2.2.2]propellane the most easily excited thermal skeletal stretch coincides with the extension of the bridgehead bond. The symmetric relaxation of the density will increase in intensity along with the bond extension as the energy of the HOMO will undergo an accompanying increase and $\Delta\epsilon$ for the excitation a corresponding decrease. In [1.1.1]propellane on the other hand, the most easily excited thermal stretch is the antisymmetric skeletal motion, which increases the amount of charge density in the bridgehead binding region, leading to a shortening and strengthening of this bond. This partially accounts for the observation that [1.1.1]propellane is less susceptible to thermolysis than [2.2.2]propellane, the activation energies being 30 and 22 kcal/mol, respectively.[52] In addition, both the static and the dynamic properties of the charge distribution for

[1.1.1]propellane account for the fact that this molecule is susceptible to acetolysis, while the same properties for the [2.2.2] molecule dictate that it be unreactive.

The ellipticity of the bridgehead bond in [2.1.1]propellane is so great and the charge distribution so close to the formation of a singularity and rupture of the bond that the instability present in the static distribution dominates the properties of this molecule. This molecule, in fact, does not survive above a temperature of 50 K.[75] In [2.2.1]propellane the symmetric transition density is lowest in energy and of moderate relative intensity, and this fact, coupled with the relatively large ellipticities of all three bonds of the three-membered ring in this structure, may be used to rationalize its observed thermal instability, which is similar to that observed for the [2.1.1] molecule.

Figure 6 also gives the orbital ordering for bicyclo[1.1.0]butane, another molecule which exhibits a very intense low-frequency absorption.[74] The bonding and antibonding characters of the HOMO and of the symmetric and antisymmetric virtual orbitals are the same as in the propellanes. The excitation energies for the SS and AS transition densities are close in value, with the SS density lying lowest. While the symmetric motion is predicted to be slightly favored in terms of the $\Delta\epsilon$ values, it is clear from the contour plot for ρ_{SS} that it will be of low intensity, because the dipolar component of this transition density is small and tends to cancel out. The transition dipole arising from the ρ_{AS} transition density is, however, very large, and the antisymmetric bridgehead stretch of B_1 symmetry should be a very intense band. These predictions are in agreement with experiment,[74] which shows this molecule to have a weak, low lying symmetric stretch at 422 cm^{-1}

and a very strong antisymmetric stretch at 735 cm^{-1}. The chemistry of bicyclobutane, like that of [1.1.1]propellane, is dominated by the properties of the charge density in the bridgehead region. Both molecules exhibit nonbonded concentrations of charge on the bridgehead carbons, and these concentrations are enhanced by the very pronounced asymmetric polarization of the bridgehead density induced by the antisymmetric skeletal stretch.

VI. Summary

It is the purpose of this work to demonstrate that molecular structures can be assigned and their relative stabilities and reactivities understood in terms of global and local properties of the electronic charge density. In the following companion paper, the atomic *averages* of the charge and energy densities are used to account for energy additivity in the homologous series of acyclic alkanes and for the deviations from this scheme that are observed for molecules containing small ring structures, deviations which give rise to the concept of strain energy.

Theoretical Analysis of Hydrocarbon Properties. 2. Additivity of Group Properties and the Origin of Strain Energy

Kenneth B. Wiberg,[*†] **Richard F. W. Bader,*** **and Clement D. H. Lau**

Contribution from the Departments of Chemistry, Yale University, New Haven, Connecticut 06511, and McMaster University, Hamilton, Ontario, L8S 4M1 Canada. Received July 11, 1986

Abstract: The theory of atoms in molecules is used to obtain electron populations and energies for the atoms in the same set of molecules studied in the preceding paper. Hydrogen is more electronegative than carbon in hydrocarbons with no geometrical strain, and the order of the relative electron-withdrawing abilities of the groups is H > CH$_3$ > CH$_2$ > CH > C. The electronegativity of a carbon increases with an increase in geometrical strain as measured by the decrease in its bond path angles from the normal value. In cyclopropane 0.05 fewer electrons are transferred from carbon to hydrogen than in the standard CH$_2$ group. The bridgehead carbons in the propellanes and in the most strained of the bicyclic molecules withdraw charge from CH$_2$ and H, and there is a flow of charge from the peripheral groups to the bridgehead region with increasing strain in these molecules. It is found that the charge distribution of a CH$_3$ or CH$_2$ group as defined by theory can appear unchanged as a transferable unit throughout a homologous series of molecules. When this occurs, the contribution of the group to the total energy of the molecule is also unchanged, and these groups account for the additivity of energy. The transfer of charge from H to C in CH$_2$ that occurs as C is subjected to geometric strain leads to a decrease in the energy of C but to an even greater increase in the energy of H, and the net result is a strain energy equal to the increase in energy of CH$_2$ relative to that of the standard. The more strained a bridgehead carbon, the greater its stability relative to its neighboring groups from which it withdraws charge, causing their energies to increase above the standard values and thereby resulting in a strain energy.

I. Introduction

This paper illustrates the relationship between the spatial form of an atom and its properties. In particular, it is demonstrated that when the distribution of charge over an atom or some functional group is the same in two different molecules, then the atom or group makes the same contribution to the total energy in both systems.[1] This property of an atom is exemplified for the homologous series of acyclic hydrocarbons whose experimental heats of formation exhibit group additivity.[2] The atomic properties are also used to obtain an understanding of the closely related quantity of strain energy.[3] This energy is defined in terms of the difference between the observed heat of formation and that predicted on the basis of group additivity. The same sets of acyclic,

[†] Yale University.

(1) Bader, R. F. W.; Beddall, P. M. *J. Chem. Phys.* 1972, *56*, 3320.
(2) Franklin, J. L. *Ind. Eng. Chem.* 1949, *41*, 1070.
(3) Wiberg, K. B. *Angew. Chem., Int. Ed. Engl.* 1986, *25*, 312.